

***Interactive comment on “Evidence of intense climate variation and reduced ENSO activity from  $\delta^{18}\text{O}$  of *Tridacna* 3700 years ago” by Yue Hu et al.***

*Anonymous Reviewer #1:*

*We would like to thank this reviewer for her/his professional comments on our manuscript. Please find our detailed answers to each comment below. The reviewer comments are in normal black script, our answers are in blue italics and the revised texts are in blue normal script.*

The data presented is of high quality and the method is robust.

A lower frequency but larger amplitude of ENSO events is found 3700 years ago, which is very interesting.

However, the authors find a larger variability (estimated by the standard deviation) of temperature anomalies in the fossil record and yet conclude (including in the title) for a reduced activity of ENSO at that time. The "activity" of ENSO is a widely used but poorly defined term that includes both frequency and amplitude. The standard deviation of interannual SST anomalies also integrates frequency and amplitude of events and is therefore usually used as an estimate of ENSO activity.

This means that the conclusion should not point to a reduced activity of ENSO but to an increased activity, or, more precisely, to an increased ENSO-related variability in this region.

*Thank you for your professional suggestion. We have corrected the “reduced ENSO activity” into “reduced ENSO frequency”, and use “ENSO-related variability” to indicate the standard deviation of interannual SST anomalies. The conclusion has also corrected.*

The contrast with reconstructions from the eastern Pacific (Koutavas et al., 2012, Carré et al., 2014) may point to interesting changes in ENSO flavours.

*It is really interesting to find an opposite conclusion on the other side of the Pacific on the same time-scale. We have added sentences to discuss this contrast in the last part of 4.4:*

*As a result, the enhanced climate variability 3700 years ago probably indicates increased ENSO-related variability in this region. This conclusion contradicts data from samples (deep-sea sediments and fossil mollusk shells) collected in the eastern tropical Pacific at the same time period (Koutavas et al., 2012, Carré et al., 2014). More data should be analyzed from long, successive time periods to understand more about the dynamics of ENSO on a large scale.*

The paleo-ENSO literature seems not completely understood. Some references are sometimes not properly cited. Tudhope et al. 2001, for instance is once cited to support decreased variability at 3.7ka and somewhere else for the opposite.

*We apologize for this mistake. We have checked and corrected them in revision.*

.

The english still needs to be improved.

*We have asked an English language editor for help to improved our manuscript this time, who have worked in CP copy-editing services before, and hope it's better than before for you to comprehend our study.*

The original isotopic data of modern and fossil shells should be included as supplementary material, or available in a public repository such as Pangaea.

*We have added the supplementary material of both shells. The isotopic data of Modern shell are in Table S1, the data of fossil shell are in Table S2.*

***Interactive comment on “Evidence of intense climate variation and reduced ENSO activity from  $\delta^{18}\text{O}$  of *Tridacna* 3700 years ago” by Yue Hu et al.***

*Anonymous Reviewer #2:*

*We would like to thank this reviewer for her/his comments on our manuscript. Please find our detailed answers to each comment below. The reviewer comments are in normal black script, our answers are in blue italics and the revised texts are in blue normal script.*

General comments:

I can see from their comments and corrections in the manuscript that Hu et al. have made great efforts to accommodate all reviewer suggestions and this has greatly improved the manuscript. However, I have three objectives that I feel need to be addressed before this manuscript can move forward:

Firstly, the writing has still many language issues (especially the new yellow text passages) and I would like to urge the authors to seek some editorial support either through the journal or within their professional network. I believe it is not the reviewer's job to correct the entire grammar of a manuscript but to evaluate and support the intellectual achievement. I will do my best to provide some additional language help but need to emphasise here that this is just scratching the surface. Also, missing line numbers in the most recent version make it very difficult to provide specific comments.

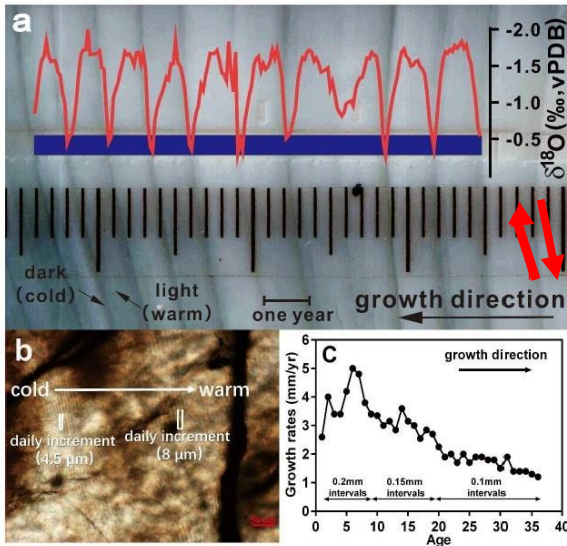
*Thank you for your additional language help to us. We have asked an English language editor for help to improve our manuscript once again, and hope it's better than before for you to comprehend our study. Also, line numbers are added to the manuscript.*

Secondly, I am still not convinced that fastest growth rates correlate with warm seasons. It could be the case but (in theory) it's a 50/50 chance so you need to demonstrate this clearly. I understand that it may be challenging to visualise them from the fossil shell but why don't you use your modern shell for this? I assume you know when the shell was collected and sacrificed (summer or winter) you could prepare a microscope image showing the inner growth front and check if a dark or bright (opaque) line was formed most recently. There shouldn't be any interfering organic matter in this sample. I believe this extra effort could go a long way and

greatly support your argumentation with direct evidence.

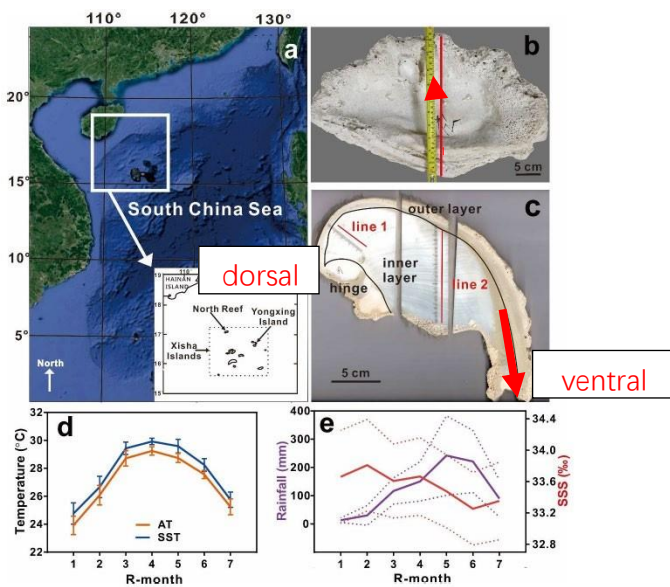
*Your suggestion about using the modern shell is really good to support our argumentation. In fact, we do use a modern Tridacna, collected in Xisha Islands with an accurate daily time-scale, to analyze the growth rate change under daily increments by using laser scanning confocal microscope. The result shows it is true that Tridacna from Xisha Islands grows fast in warm while relative slow in cold temperature. However, this paper is accepted by PNAS and will be published soon. We apologize here that we cannot cite right now.*

Lastly, I believe the arrow indicating the direction of growth in Figure 3 has a wrong orientation and it is missing in Figure 1 altogether. Such shell orientation “landmarks” are important and need to be presented for the reader to understand the shell geometry. A growth direction arrow always refers to the dorso-ventral shell extension and, thus, will never be perpendicular to the growth lines of an inner shell layer (as in this case for the inner layer of *Tridacna* here). It will be roughly parallel to these growth lines – as the inner surface of the shell is not depicted in this image there are 2 options  
– it could be pointing up or downwards (as indicated by my red arrows). Authors need to check where on the section they took the image and re-draw the arrow accordingly. Alternatively for Figure 3 authors could consider leaving the arrow as it is but modify the text to read “local direction of growth”, then this arrow would indeed indicate the orientation of the inner shell layer (instead of the dorso-ventral growth direction, see Otter et al 2019 for more explanation on shell growth directions).



Growth direction  
(defined as dorso-ventral  
shell extension)

I have also inserted direction of growth arrows in Figure 1 for the authors as they should consider adding it to their figure (smaller and black of course I exaggerate here just for the purpose of clarity). For further information on the difference in general and local shell growth directions I recommend reading and citing Otter et al. "Insights into architecture, growth dynamics, and biomineralization from pulsed Sr-labelled *Katelysia rhytiphora* shells (Mollusca, Bivalvia)." *Biogeosciences* 16.17 (2019): 3439-3455, especially chapter 3.6.



*Thank you for your professional advice. We have added more details of shell geometry in our figures refer to Gannon et al. (2017).*

*Besides, we apologize for making confusion about the word "growth direction". We know the *Tridacna* grow its whole shell from that you demonstrate, but what we want to express is the direction that *Tridacna* precipitates its shell from young to old. According to Gannon et al. (2017), who study the biomineralization of Indo-Pacific giant clam *Tridacna gigas*, indicate the mineralization of the inner and outer layers is independent from each other and associated with the activity of specific mantles. From Fig. 1 in their*

research, the layers are different between inner and outer. We acquire our sample of inner layers from the growth of young to old, and each sample is parallel with the layer. We have removed the word “growth direction” into the word “growth (young to old)” to avoid confusion. Also, we have added the description of the shell in 2.2.

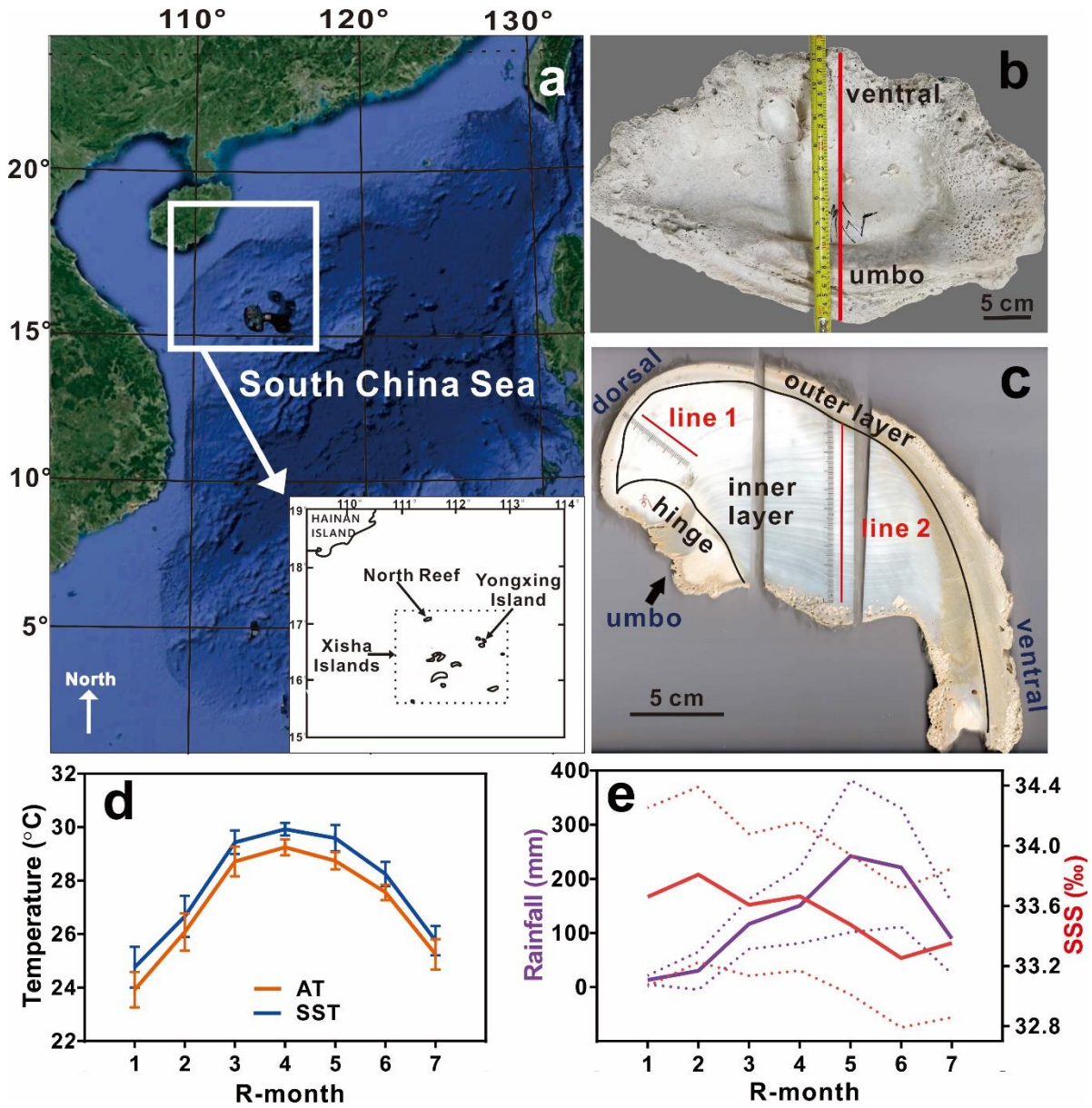


Figure 1

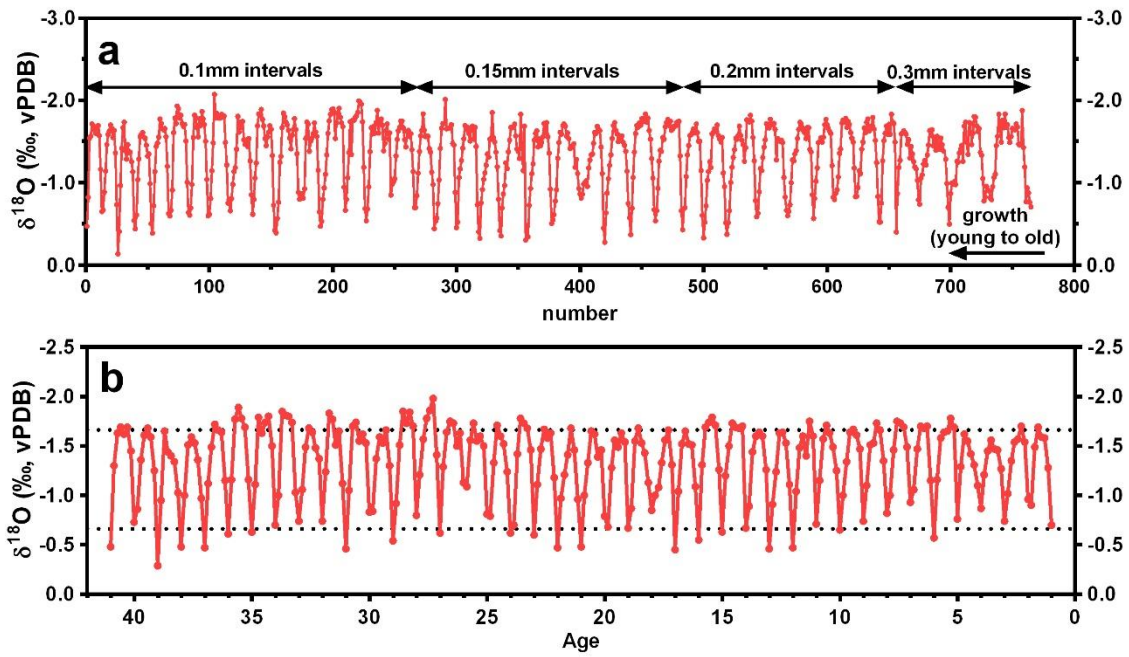


Figure 2

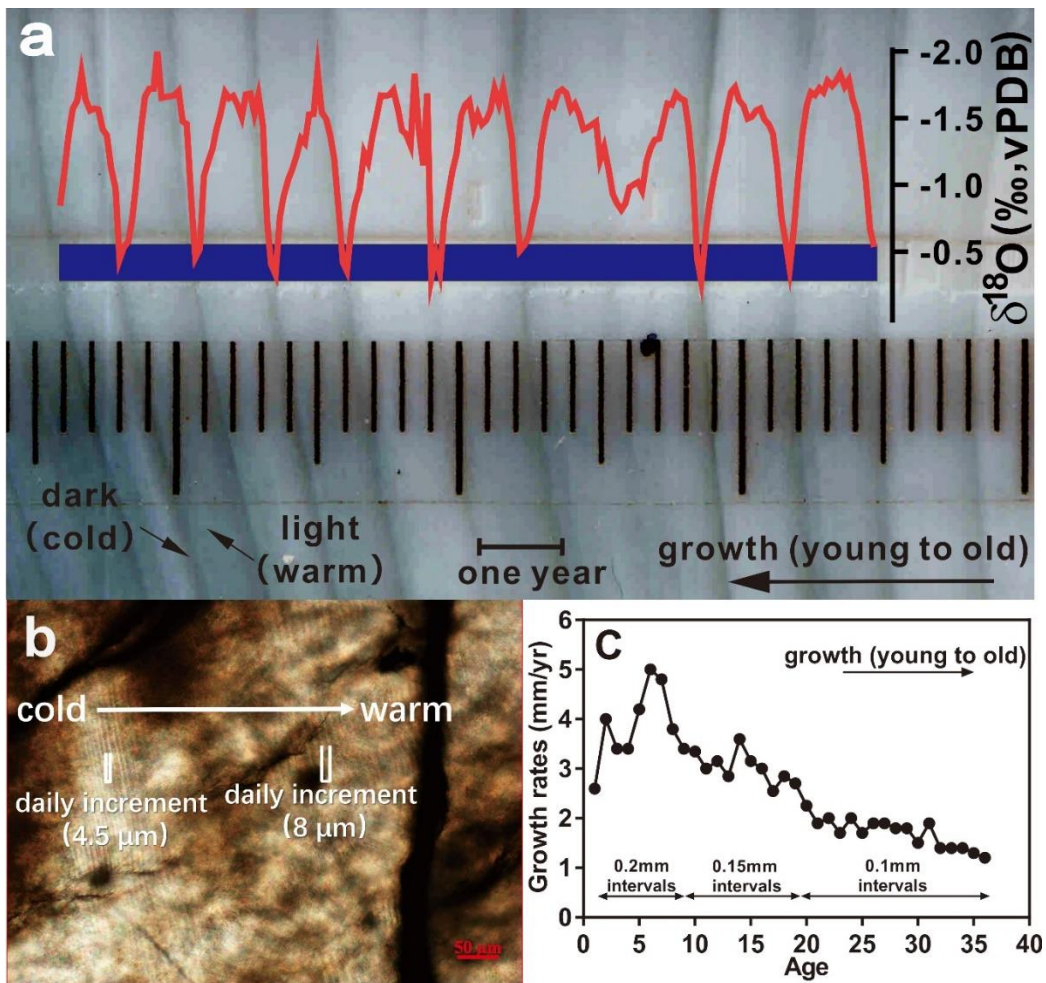


Figure 3

I hope this second round of suggestions does not discourage the authors and hope they can view these comments as a last “fine tuning” of their manuscript and hope they will undertake this last effort. I look forwards to seeing the final published version of this study!

*We appreciate your careful and detailed suggestions for our manuscript. We will do our best to make it more professional! Thank you again!*

Specific comments:

**Abstract:**

omit “in the tropical ocean” as Tridacna is the largest bivalve in general.

*Done.*

**Introduction:**

delete “and ontogenetic” as this reads confusing (they do not help to understand past climate it is just an intrinsic growth pattern of the animals).

*Done.*

“Bivalves, which are considered to be high-resolution records, can give us more precisely environmental variation details.” Change to “Bivalve shells” as the soft tissue is not used.

*Done.*

“Studies in bivalve mollusk specimen (*Arctica islandica*) oxygen isotopes showed a different seasonal temperature change compared between the Little Ice Age and the present” it is not clear what you mean with this sentence and why you give this information. These literature examples need to be better embedded within your story. Why is this relevant?

*Another referee suggests us to add some researches about other bivalves. We have rewrote*



*this sentence and changed it into the forth paragraph of introduction. We want to emphasize the high-resolution isotopic data in other bivalves have been paid attention, then indicate that Tridacna can provide high-resolution details as well.*

“Previous studies indicated that Tridacna species grow their shells with the oxygen isotopic ( $\delta^{18}\text{O}$ ) equilibrium with seawater” change to “Previous studies indicated that Tridacna grow their shells in oxygen isotopic ( $\delta^{18}\text{O}$ ) equilibrium with the surrounding seawater” and better end the sentence after the provided references and modify beginning of next sentence.

*We have corrected those sentences.*

Check for past and present tenses: “...studies on the mid to late Holocene ENSO evolution yield controversial findings” and “Coral records show” “fossil mollusk shells suggest” Ask yourself do they still show? Is it still the case? Then use present tense when speaking about earlier findings.

*Thank you! We have corrected them.*

### **Materials and methods:**

“Due to suggested in the method (Schöne and Fiebig, 2009) and the yearly minimum number of  $\delta^{18}\text{O}_{\text{YX1}}$  was seven, the time-scale of modern Tridacna YX1 is resampling into seven points/yr, which indicates a resampled month (r-month) represents 1.7 actual month. All meteorological observations and  $\delta^{18}\text{O}_{\text{shell}}$  are using this method to resample the time-scale” needs to be rewritten for clarity (grammar).

*We have rewrote this paragraph into:*

In order to compare geochemical analyses with monthly environmental data, isotopic records and meteorological observations were resampled according to the method suggested by Schöne and Fiebig (2009). They used bivalve shells (*Arctica islandica*) to reconstruct the climate, examining seven points per year would minimize the influence of

different growth rates throughout the year; meanwhile, only the annual sample number for which equal to or more than seven existed could be used. As the yearly minimum number of  $\delta^{18}\text{O}_{\text{YX1}}$  is seven, 1 year includes 7 resampled months (r-months).

“Study in shell architecture showed a crossed lamellar microstructure with a strong fibre texture made the mechanical properties of those bivalve shells more optimized (Agbaje et al., 2017)” perhaps change to “A recent study investigating the architecture of Tridacna shells shows a crossed lamellar microstructure with a strong fibre texture with optimised mechanical performance (Agbaje et al., 2017).”

*Done.*

...performed at the Institute of Earth Environment of the Chinese...” and “the fossil Tridacna gigas age is 3437...”

*Done.*

“...the standards and samples had reproducibilities ( $1\sigma$ ) of better...”

*Done.*

The last paragraph of the methods section needs more extensive language editing.

*We have polished this paragraph and hope it will be better for you to comprehend.*

## **Results**

“From the shell section” (delete slice)

*Done.*

“...which suggests *Tridacna* grew in low temperature (potentially from December to February).” And “In contrast, lower  $\delta^{18}\text{O}_{\text{A5}}$  values lie in the wider bright, opaque lines...” careful with the word “lighter” this refers to density and weight – what you mean is “brighter” – check and edit throughout the manuscript.

*Thank you for your suggestion. We have changed this word throughout the manuscript.*

“Furthermore, daily increments visible as pairs of dark and bright increments can be seen...”

*Done.*

“This period fell into the cold season with daily increments of about 2.7  $\mu\text{m}$  width.” You mean one dark and bright pair?

*We apologize for wrong numbers here. The “2.7” and “5.7” are the number before we retreated the picture Fig. 3b. After the retreatment, a new clearer daily increment was measured. The correct phrases should be:*

*This period fell during the cold season, when the daily growth increment was about 4.5  $\mu\text{m}$ . When the temperature rose as warm season began, *Tridacna* grew faster, with daily growth increment reaching up to 8  $\mu\text{m}$ .*

### **Discussion:**

“R-monthly mean values are used to compare for they are minimizing the influence of extreme events.” It is not clear what you mean – what do you compare?

*We want to use mean r-monthly values of  $\delta^{18}\text{O}_{\text{YXI}}$ ,  $\delta^{18}\text{O}_{\text{SST}}$ , and  $\delta^{18}\text{O}_{\text{SSS}}$  to do the comparison. This sentence has rewrote:*

*For the purpose of minimizing the influence of extreme values, mean r-monthly  $\delta^{18}\text{O}$  profiles ( $\delta^{18}\text{O}_{\text{YXI}}$ ,  $\delta^{18}\text{O}_{\text{SST}}$ , and  $\delta^{18}\text{O}_{\text{SSS}}$ ) are used to compare.*

Perhaps better: “As ENSO is the strongest contributor to global interannual climate variations a better understanding of its fundamental properties will allow us to better unravel past climate change episodes and to make more accurate predictions for the future”

*Thank you. We have rewrote this sentence as your advice.*

### *References*

Gannon, M. E., Pérez-Huerta, A., Aharon, P. and Street, S. C.: A biomineralization study of the Indo-Pacific giant clam *Tridacna gigas*, *Coral Reefs*, 36(2), 503–517, doi:10.1007/s00338-016-1538-5, 2017.

# Evidence from giant clam $\delta^{18}\text{O}$ of intense El Niño–Southern Oscillation-related variability but reduced frequency 3700 years ago

Yue Hu<sup>a,b</sup>, Xiaoming Sun<sup>a,b,c,d\*</sup>, Hai Cheng<sup>e,f</sup>, Hong Yan<sup>g,h,i\*</sup>

<sup>a</sup> School of Marine Sciences, Sun Yat-sen University, Guangzhou 510006, China

<sup>b</sup> Guangdong Provincial Key Laboratory of Marine Resources and Coastal Engineering, Guangzhou 510275, China

<sup>c</sup> School of Earth Sciences and Engineering, Sun Yat-sen University, Guangzhou 510275, China

<sup>d</sup> Southern Marine Science and Engineering Guangdong Laboratory (Zhuhai), Zhuhai 519000, China

<sup>e</sup> Institute of Global Environmental Change, Xi'an Jiaotong University, Xi'an 710054, China

<sup>f</sup> Department of Earth Sciences, University of Minnesota, Minneapolis, Minnesota 55455, USA

<sup>g</sup> State Key Laboratory of Loess and Quaternary Geology, Institute of Earth Environment, Chinese Academy of Sciences, Xi'an 710061, China

<sup>h</sup> CAS Center for Excellence in Quaternary Science and Global Change, Xi'an 710061, China

<sup>i</sup> OCCES, Qingdao National Laboratory for Marine Science and Technology, Qingdao 266061, China

\*Corresponding authors: eessxm@mail.sysu.edu.cn; yanhong@ieecas.cn

## Abstract

Giant clams (*Tridacna*) are the largest marine bivalves, and their carbonate shells can be used for high-resolution paleoclimate reconstructions. In this contribution,  $\delta^{18}\text{O}_{\text{shell}}$  was used to estimate climatic variation in the Xisha Islands of the South China Sea. We first evaluate sea surface temperature (SST) and sea surface salinity (SSS) influence on the modern resampled monthly (r-monthly) resolution of *Tridacna gigas*  $\delta^{18}\text{O}_{\text{shell}}$ . The results obtained reveal that  $\delta^{18}\text{O}_{\text{shell}}$  seasonal variation is mainly controlled by SST and appears to be insensitive to local SSS change. Thus, the  $\delta^{18}\text{O}$  of *Tridacna* shells can be roughly used as a proxy of local SST: a 1 ‰  $\delta^{18}\text{O}_{\text{shell}}$  change is roughly equal to 4.41 °C of SST. The r-monthly  $\delta^{18}\text{O}$  of a 40-year-old *Tridacna squamosa* (3673 ± 28 BP) from the North Reef of the Xisha Islands was analyzed and compared with the modern specimen. The difference between the average  $\delta^{18}\text{O}$  of the fossil *Tridacna* shell ( $\delta^{18}\text{O} = -1.34$  ‰) and the modern *Tridacna* specimen ( $\delta^{18}\text{O} = -1.15$  ‰) probably implies a warm climate, roughly

34 0.84°C, in 3700 years ago. The seasonal variation 3700 years ago was slightly lower than that  
35 suggested by modern instrumental data, and the transition between warm and cold seasons was rapid.  
36 Higher amplitudes of reconstructed r-monthly and r-annual SST anomalies imply an enhanced  
37 climate variability during this warm period. Investigation of the El Niño–Southern Oscillation  
38 (ENSO) variation (based on the reconstructed SST series) indicates reduced ENSO frequency but  
39 increased ENSO-related variability and extreme El Niño winter events 3700 years ago.

40

41 **Keywords:** *Tridacna*;  $\delta^{18}\text{O}$ ; South China Sea; Seasonal variation; Climate variation; ENSO activity

42

## 43 1 Introduction

44 The carbonate skeletons of marine organisms, such as corals, foraminifers, and mollusks, have  
45 been widely used to reconstruct environmental variation (Aharon, 1983; Batenburg et al., 2011;  
46 Ourbak et al., 2006; Schöne et al., 2005; Wanamaker et al., 2011; Yoshimura et al., 2016; Yu et al.,  
47 2005). Due to their high sensitivity to the surrounding environment and that they preserve high-  
48 resolution biochemical variations in their skeleton, these marine biogenic carbonates can shed light  
49 on past climate dynamics. Bivalves, which are considered to be high-resolution records, can give us  
50 more precise details on environmental variation. Giant clams (*Tridacna*), as they are the largest  
51 bivalves and usually live in tropical coral reefs, have received increasing scientific attention in  
52 recent decades (Pätzold et al., 1991; Watanabe et al., 1999; Watanabe et al., 2004; Elliot et al., 2009;  
53 Ayling et al., 2015; Agbaje et al., 2017). This is because their shells have many favorable properties  
54 for recording local environmental changes: they have dense and well-preserved aragonite shells,  
55 fast growth rates (up to 1 cm per year) with clear annual growth lines, and a longevity of several  
56 decades to about 100 years. These characteristics allow *Tridacna* to provide ideal material for high-  
57 resolution reconstruction of interannual, seasonal, or even sub-seasonal climatic variations.

58 Previous studies indicate that *Tridacna* species grow their shells in oxygen isotopic ( $\delta^{18}\text{O}$ )  
59 equilibrium with the surrounding seawater (Aharon, 1991; Aharon and Chappell, 1986; Pätzold et  
60 al., 1991; Romanek and Grossman, 1989; Watanabe et al., 1999). The reliability of reconstructing  
61 temperature and seawater  $\delta^{18}\text{O}$  variability is not reduced and does not show obvious increasing or  
62 decreasing trends due to *Tridacna*'s ontogenetic growth of the *Tridacna* (Welsh et al., 2011). These  
63 studies imply that  $\delta^{18}\text{O}_{\text{shell}}$  can be used to reconstruct late Quaternary sea-level and climatic changes.  
64 Indeed, the  $\delta^{18}\text{O}$  of marine biogenic carbonates is not only influenced by sea surface temperature  
65 (SST), but also by surrounding seawater  $\delta^{18}\text{O}$ . Meanwhile, seawater  $\delta^{18}\text{O}$  has a close correlation  
66 with sea surface salinity (SSS), which is affected by tropical evaporation and the precipitation  
67 balance. Nonetheless, the influence of SST and SSS on  $\delta^{18}\text{O}_{\text{shell}}$  is unclear due to the distinct  
68 variation of temperature and salinity in different areas. For example, the  $\delta^{18}\text{O}_{\text{shell}}$  of *Tridacna* from  
69 southwestern Japan can be directly used as a proxy of SST (Yamanashi et al., 2016), while the

70  $\delta^{18}\text{O}_{\text{shell}}$  of Indonesian *Tridacna* has been interpreted to be a contributed of 71.4 % from SST and  
71 28.6 % from SSS (Arias-Ruiz et al., 2017). Thus, local calibration from modern *Tridacna* is  
72 important in determining the relationship of  $\delta^{18}\text{O}_{\text{shell}}$ , SST, and SSS.

73 Climatic variation in the Meghalayan (which began 4200 BP in the late Holocene) has  
74 significant impacts on human society and ecosystem development. However, early Meghalayan  
75 climatic conditions in SE Asia around the South China Sea still remain poorly understood. Shi (1994)  
76 reviewed data from various sources (such as ice cores, inland lakes, paleosols in loess and eolian  
77 sands, sea-level fluctuations, palynological and botanical studies) in China, and found that early  
78 Meghalayan is a part of the Holocene megathermal period (8 to 3 ka BP). Sediments in the South  
79 China Sea also imply that the temperature might have been relatively higher in the early Meghalayan  
80 than in the present (Ouyang et al., 2016). However, these studies are low-resolution, and high-  
81 resolution records under interannual climate variation are rare. With global warming and numerous  
82 climatic disasters happening in recent decades, climatic conditions in early Meghalayan could serve  
83 as an analogue to modern problems, and have received increasing scientific attention (Schirmacher  
84 et al., 2019; Scuderi et al., 2019; Toth and Aronson, 2019; Zhang et al., 2018). Recent studies of  
85 bivalve mollusk specimen (*Arctica islandica*) oxygen isotopes show high-resolution data with  
86 seasonal signals (Schöne et al., 2005; Wanamaker et al., 2011). High-resolution isotopic  
87 geochemical data from *Tridacna* may also provide detailed insight into climatic variations in early  
88 Meghalayan.

89 Furthermore, El Niño–Southern Oscillation (ENSO) is widely accepted as the main source  
90 of interannual climatic variability in the Pacific Ocean. Previous studies suggest that the impacts of  
91 ENSO activity are not limited to tropical areas, but might also apply to global atmospheric  
92 circulation through the heating-up of the tropical atmosphere (Cane, 2005). Thus, reconstructing  
93 ENSO is very important for understanding its dynamics and predicting future change. Many early  
94 studies on ENSO behaviors were constructed with low-resolution proxy data using deposition  
95 events (Rodbell et al., 1999; Koutavas and Joanides, 2012) or ice cores (Thompson et al., 1995; 1998)  
96 in order to reveal ENSO variance over thousands of years. However, the periodicity of ENSO is  
97 short, making it difficult to use these low-resolution data to precisely determine the strength and  
98 variability of ENSO activity. Recent studies focus on seasonal or monthly data to examine precise  
99 variation of ENSO activity (Arias-Ruiz et al., 2017; Ayling et al., 2015; McGregor et al., 2013;  
100 Welsh et al., 2011; Yan et al., 2017), but those fragmental data cannot fully explain the Holocene  
101 ENSO dynamics. Therefore, fragments from different times according to different high-resolution  
102 samples are needed and can provide an integrated framework for examining ENSO theory and  
103 models of the Holocene. In addition, studies on the middle to late Holocene ENSO evolution yield  
104 controversial findings: coral records show a reduced ENSO variability around early Meghalayan  
105 (Tudhope et al., 2001; McGregor et al., 2013; Cobb et al., 2013; Woodroffe et al., 2003). Other  
106 carbonate species like fossil mollusk shells suggest that ENSO variance was severely damped ~4000

107 years ago (Carré et al., 2014). Yet other studies indicate strengthening ENSO activity at 4 to 3 ka  
108 (Duprey et al., 2014; Yang et al., 2019). Thus, this further points to the importance of high-resolution  
109 isotopic geochemical data such as from *Tridacna* in unraveling the dynamics of ENSO.

110 This study aims to evaluate seasonality, climate variation, and ENSO activity in the Xisha  
111 Islands of the northern South China Sea, based on two high-resolution  $\delta^{18}\text{O}_{\text{shell}}$  profiles of modern  
112 and fossil *Tridacna*. The study area is situated in the northwest margin of the west Pacific warm  
113 pool (WPWP), and the local climate is widely accepted to be directly responsive to ENSO activity  
114 (Mitsuguchi et al., 2008; Yan et al., 2010). A modern *Tridacna gigas* shell was first used to estimate  
115 the extent of environmental control (SST and SSS) on  $\delta^{18}\text{O}_{\text{shell}}$ , and a new SST- $\delta^{18}\text{O}_{\text{shell}}$  linear  
116 regression was proposed. Subsequently, a fossil *Tridacna squamosa* (which lived to 40 years) was  
117 used to reconstruct seasonality and climatic variation, and the obtained results are compared with  
118 the modern species and meteorological observations. Finally, ENSO activity and extreme El Niño  
119 winter events were discussed, using the re-established SST anomalies.

120

## 121 2 Materials and methods

### 122 2.1 Regional setting

123 The South China Sea is located in the northwest of WPWP (Fig. 1a), and its interannual  
124 climate is closely related to ENSO activities (Mitsuguchi et al., 2008; Yan et al., 2010). The Xisha  
125 Islands in the northern South China Sea is substantially influenced by two contrasting Asian  
126 monsoons from opposite directions: the Asian summer monsoon from the southwest and the Asian  
127 winter monsoon from the northeast. These two monsoons provide distinct seasonal SST for the  
128 *Tridacna* populating the coral reefs of the Xisha Islands. Our sample (*Tridacna squamosa* A5) was  
129 collected in the North Reef (17°05' N, 111°30' E), whilst the modern *Tridacna gigas* sample YX1  
130 (studied previously by Yan (2013)) was acquired from Yongxing Island (16°50' N, 112°50' E),  
131 which is about 90 kilometers away from the North Reef (Fig. 1b).

132 Meteorological observations (atmosphere temperature, AT; SST; SSS; rainfall) were obtained  
133 from the Institute of Meteorology of China, which has taken records for the Xisha Islands since  
134 1958. In order to compare geochemical analyses with monthly environmental data, isotopic records  
135 and meteorological observations were resampled according to the method suggested by Schöne and  
136 Fiebig (2009). They used bivalve shells (*Arctica islandica*) to reconstruct the climate, examining  
137 seven points per year would minimize the influence of different growth rates throughout the year;  
138 meanwhile, only the annual sample number for which equal to or more than seven existed could be  
139 used. As the yearly minimum number of  $\delta^{18}\text{O}_{\text{YX1}}$  is seven, 1 year includes 7 resampled months (r-  
140 months). Figure 1d shows the r-monthly average time series of AT, SST, SSS, and rainfall, and their  
141 standard deviations (SDs). The mean SST is 27.77 °C, and AT shows a highly positive correlation  
142 with SST ( $r = 0.98$ ), but is about 0.7 °C lower. The SST seasonality is 5.33 °C, with the lowest value  
143 and highest value occurring in first and fourth r-months, respectively. It is excluded that river runoff



144 effects on SSS as the Xisha Islands are about 300 km away from the continent (Hainan Island). SSS  
145 vary from 33.25 to 33.81 ‰, and the change is mainly dominated by rainfall: higher SSS in dry  
146 winters and lower SSS in wet summers (Fig. 1e).

147 The SST data in the North Reef are acquired from NOAA HadISST, a global monthly SST data  
148 with a spatial resolution of  $1 \times 1^\circ$  (data grid cell includes both the North Reef and Yongxing Island)  
149 from 1982 to 2017. Niño 1 + 2 SST data are obtained from NOAA monthly data between 1982 and  
150 2017 (<http://www.cpc.ncep.noaa.gov/data/indices/sstoi.indices>; last access: 31/12/2017).

## 151 2.2 Shell descriptions and sample preparation

152 The original fossil *Tridacna* was cut from the umbo to the ventral (red line in Fig. 1b), where  
153 the thickness of the inner layer is the greatest. From the slice we cut, the fossil *Tridacna* has three  
154 different zones (Fig. 1c): the inner layer, the outer layer and the hinge. A recent study investigating  
155 the architecture of *Tridacna* shells shows a crossed lamellar microstructure with a strong fibre  
156 texture with optimized mechanical performance (Agbaje et al., 2017), and the mineralization of  
157 inner layer and outer layer is independent from each other (Gannon et al., 2017). The inner layer is  
158 chosen for the analyses because of its clear growth layer and well-preserved shell. Published data  
159 also reveal that inner layer  $\delta^{18}\text{O}$  values are unaffected by ontogeny (Welsh et al., 2011), and could  
160 better reflect actual  $\delta^{18}\text{O}$  than the outer layer or the hinge (Pätzold et al., 1991; Elliot et al., 2009).

161 The determination of radiocarbon age performed at the Institute of Earth Environment of  
162 Chinese Academy of Sciences. The  $^{14}\text{C}$  accelerator mass spectrometry data revealed that the fossil  
163 *Tridacna gigas* age is  $3437 \pm 28$  yr BP. Due to the lack of an obvious “reservoir effect” in the dating  
164 results of modern *Tridacna* shells, the atmospheric  $^{14}\text{C}$  yield model is used to calibration (Liu et al.,  
165 2019). The calibrated date ( $2\sigma$ ) range from 3733 to 3613 cal BP, with the median date is 3691 cal  
166 BP by using the IntCal13 of Radiocarbon Calibration Program CALIB 7.10. (<http://calib.org>). Both  
167 X-ray diffraction (XRD) and laser Raman spectrometers results show aragonite, and no other  
168 substances are found.

## 169 2.3 Stable isotopes

170 Each stable isotope sample was micromilled parallel to the growth layer with 1 mm long and  
171 100  $\mu\text{m}$  deep under a micro-drill automated system (Micro-Drill New Wave Research, Olympus SZ  
172 61) in the Isotope Laboratory of Xi’an Jiaotong University, China. Four intervals were used  
173 according to the growth rates: 100  $\mu\text{m}$  ( $n = 1$  to 268), 150  $\mu\text{m}$  ( $n = 269$  to 481), 200  $\mu\text{m}$  ( $n = 482$  to  
174 657), and 300  $\mu\text{m}$  ( $n = 658$  to 765) respectively in a transect from adult to ontogenetically younger  
175 shell (Fig. 2a).

176 The  $\delta^{18}\text{O}$  of the *Tridacna* was analyzed in the Isotope Laboratory of Xi’an Jiaotong University,  
177 using the ThermoFinnigan MAT-253 mass spectrometer fitted with a Kiel Carbonate Device IV. All  
178 results were reported in per mil (‰), relative to the Vienna PeeDee Belemnite (VPDB) standard.  
179 The standard GBW04405, which has been compared with international standard NBS-19, was  
180 added to the analyses every 10 to 20 samples to check reproducibility. The average value of standard

181 powder in  $\delta^{18}\text{O}$  is  $-8.49 \pm 0.14$  ‰. Duplicate measurements of GBW04405 standards and samples  
182 showed long-term reproducibilities ( $1\sigma$ ) of less than 0.14 ‰ and 0.05 ‰, respectively.

183 Published data of the modern *Tridacna gigas* shell YX1 were used to investigate the  
184 relationship between *Tridacna*  $\delta^{18}\text{O}$  and the local climate (Yan et al., 2013). YX1 was collected from  
185 Yongxing Island, 90 km ESE of the North Reef (Fig. 1b). The internal carbonate standard of modern  
186 *Tridacna* YX1  $\delta^{18}\text{O}$  (VPDB) was also GBW04405; the standards and samples had reproducibilities  
187 ( $1\sigma$ ) of better than 0.08 ‰ and 0.06 ‰, respectively.

#### 188 2.4 Data processing and analyses

189 PearsonT3 (Version 2.2, January 2017) was used to test the correlation coefficient. Successive  
190 sets of 100 years' length were calculated to estimate monthly insolation using the software  
191 AnalySeries 2.0.8 (Laskar et al., 2004), which contained the probable life span of *Tridacna* (A5) as  
192 considering  $2\sigma$  confidence intervals of corrected age. The timescale of modern insolation ranges  
193 from 1918 to 2017, while the past ranges from 3722 to 3623 BP. Statistical analyses performed with  
194 the software Origin 2018 and PAST (Paleontological Statistics) 3.18. The isotopic records,  
195 meteorological observations and insolation data were resampled for seven points per year using the  
196 software AnalySeries 2.0.8, as used for other studies in Sclerochronology (Schöne and Fiebig, 2009;  
197 Wanamaker et al., 2011).

198

### 199 3 Results

#### 200 3.1 $\delta^{18}\text{O}_{\text{A5}}$ record

201 Seasonal cycles are distinct in the  $\delta^{18}\text{O}_{\text{A5}}$  profile (Fig. 2, Table S2), which indicate that this  
202 *Tridacna* lived for 40 years. The  $\delta^{18}\text{O}_{\text{A5}}$  range from -2.07 to -0.14 ‰ (mean -1.35 ‰, n=765). After  
203 resampling into 7 points per year,  $\delta^{18}\text{O}_{\text{A5}}$  varied from -1.98 to -0.29 ‰ (mean -1.34 ‰, n=281).

#### 204 3.2 Sclerochronology

205 From the shell section, dark/bright line couples (each couple represents 1 year) can be seen  
206 clearly (Fig. 3a). Following the  $\delta^{18}\text{O}_{\text{A5}}$  profiles, these short, dark lines (transparent) correspond to  
207 higher  $\delta^{18}\text{O}_{\text{A5}}$  values, which means that *Tridacna* grew in lower temperature (cold seasons such as  
208 December to February). In contrast, lower  $\delta^{18}\text{O}_{\text{A5}}$  values lie in the long bright lines (opaque),  
209 corresponding to the higher temperatures (warm seasons such as March to November). Annual  
210 growth rates can be calculated with the  $\delta^{18}\text{O}_{\text{A5}}$  seasonal cycles and interval distance (Fig. 3c). The  
211 results show that growth rates were higher when *Tridacna* A5 was young, reaching 5 mm per year.  
212 The growth then slowed down and stabilized to 1–2 mm per year after the *Tridacna* had matured  
213 (Fig. 3c). Furthermore, daily increments visible as pairs of dark and bright increments can be seen  
214 under the microscope (Fig. 3b). A fragment was chosen where  $\delta^{18}\text{O}$  values were nearly the highest  
215 in a particular year. This period fell during the cold season, when the daily growth increment was  
216 about 4.5  $\mu\text{m}$ . When the temperature rose as warm season began, *Tridacna* grew faster, with daily  
217 growth increment reaching up to 8  $\mu\text{m}$ . This situation occurred throughout the *Tridacna*'s life. In

218 general, *Tridacna* A5 grew faster in warm seasons and slower in cold seasons.

219 The SST observation in the Xisha Islands suggested that the first r-month nearly corresponds  
220 to the lowest SST. Thus, the highest  $\delta^{18}\text{O}$  of each cycle was chosen as the beginning of a year.

221

## 222 4 Discussion

### 223 4.1 Relation of SST, SSS, and $\delta^{18}\text{O}$ of modern *Tridacna*

224 Previous studies have demonstrated that *Tridacna* is in oxygen isotopic equilibrium with the  
225 surrounding seawater (Aharon, 1983; Watanabe et al., 1999), which also holds true for *Tridacna* in  
226 the South China Sea (Yan et al., 2013). Biogenic carbonate  $\delta^{18}\text{O}$  values show linear correlations  
227 with SST and seawater  $\delta^{18}\text{O}_{\text{water}}$  (Aharon and Chappell, 1986; Pätzold et al., 1991; Romanek and  
228 Grossman, 1989). The  $\delta^{18}\text{O}_{\text{shell}} - \text{SST} - \delta^{18}\text{O}_{\text{water}}$  Eq. (1) of Grossman and Ku (1986) is adopted, as it  
229 is widely used in calculations for tropical aragonite mollusk species. Meanwhile,  $\delta^{18}\text{O}_{\text{water}}$  has a  
230 positive relationship with SSS, and Eq (2), which was established using seawater in the northern  
231 South China Sea (Hong et al., 1997), is chosen to calculate. We merge Eq (1) and (2) into  $\delta^{18}\text{O}_{\text{shell}} -$   
232  $\text{SST} - \text{SSS}$  (Eq (3)) to roughly simplify the environmental control on  $\delta^{18}\text{O}_{\text{shell}}$ .

$$233 \text{SST } (^{\circ}\text{C}) = 21.8 - 4.69 (\delta^{18}\text{O}_{\text{shell}} - \delta^{18}\text{O}_{\text{water}}) \quad (1)$$

$$234 \delta^{18}\text{O}_{\text{water}} (\text{‰}) = 0.23 \times \text{SSS} - 7.58 \quad (2)$$

$$235 \text{SST } (^{\circ}\text{C}) = -13.75 - 4.69 \times \delta^{18}\text{O}_{\text{shell}} + 1.08 \times \text{SSS} \quad (3)$$

236 The  $\delta^{18}\text{O}_{\text{shell}}$  reflects a combination of SST and SSS variation. In order to quantify more  
237 precisely the relation between those factors and  $\delta^{18}\text{O}_{\text{shell}}$ , two  $\delta^{18}\text{O}$  profiles are calculated (Fig. 4a):  
238  $\delta^{18}\text{O}_{\text{SST}}$  (constant SSS but varying SST) and  $\delta^{18}\text{O}_{\text{SSS}}$  (constant SST but varying SSS). For the  
239 purpose of minimizing the influence of extreme values, mean r-monthly  $\delta^{18}\text{O}$  profiles ( $\delta^{18}\text{O}_{\text{YX1}}$ ,  
240  $\delta^{18}\text{O}_{\text{SST}}$ , and  $\delta^{18}\text{O}_{\text{SSS}}$ ) are used to compare. The results show that  $\delta^{18}\text{O}_{\text{YX1}}$ ,  $\delta^{18}\text{O}_{\text{SST}}$ , and  $\delta^{18}\text{O}_{\text{SSS}}$   
241 profiles are in the range of -0.57 to -1.52 ‰, -0.48 to -1.58 ‰, and -1.07 to -1.19 ‰, respectively.  
242 It is obviously that  $\delta^{18}\text{O}_{\text{YX1}}$  and  $\delta^{18}\text{O}_{\text{SST}}$  show the same trend and are highly correlated ( $r = 0.91$ ,  $n$   
243  $= 7$ ;  $r = 0.78$ ,  $n = 77$ ), but the variation range in  $\delta^{18}\text{O}_{\text{SSS}}$  is only 14 % of  $\delta^{18}\text{O}_{\text{YX1}}$ . Therefore, this  
244 indicates that the  $\delta^{18}\text{O}_{\text{shell}}$  in the Xisha Islands corresponds predominantly to seasonal SST variation.  
245 In addition, the calculated  $\delta^{18}\text{O}_{\text{predicted}}$  (by using both local actual SST and SSS) was used to compare  
246 with  $\delta^{18}\text{O}_{\text{YX1}}$  (Table S1). The  $\delta^{18}\text{O}_{\text{YX1}}$  and  $\delta^{18}\text{O}_{\text{predicted}}$  profiles have nearly the same mean value  
247 (1.15 ‰ and 1.14 ‰, respectively), and their positive correlation ( $r = 0.81$ ,  $n = 77$ ) indicates that  
248 the local *Tridacna* precipitates its shell in oxygen isotopic equilibrium.

249 Moreover, the comparison of predicted SST (under constant SSS and actual SSS with  $\delta^{18}\text{O}_{\text{YX1}}$ )  
250 further confirms that the SSS variation has no significant effect on the local reconstructed SST (Fig.  
251 4f). The two predicted SST values were highly similar ( $r = 0.93$ ), and they are well correlated with  
252 the actual SST ( $r_{\text{vary}} = 0.79$ ,  $r_{\text{constant}} = 0.78$ ). Thus, we can use  $\delta^{18}\text{O}_{\text{shell}}$  to roughly estimate the  
253 seasonal local SST variation, and to establish a new SST- $\delta^{18}\text{O}_{\text{shell}}$  linear regression:  $\text{SST } (^{\circ}\text{C}) = 22.69$   
254  $- 4.41 \times \delta^{18}\text{O}_{\text{shell}}$  (or  $\delta^{18}\text{O}_{\text{shell}} (\text{‰}) = -0.136 \times \text{SST} + 2.634$ ). A 1 ‰ change of  $\delta^{18}\text{O}_{\text{shell}}$  is roughly

255 equal to 4.41°C of SST. Yu (2005) summarized many published  $\delta^{18}\text{O}$ -SST slopes for another marine  
256 carbonate species, *Porites lutea* coral, and suggested that the slopes could range from -0.134 to -  
257 0.189. Corals from Hainan Island revealed good  $\delta^{18}\text{O}$  vs. SST correlation, with a linear regression  
258 slope of -0.137 (Su et al., 2006), very similar to our result (-0.136). Consequently, use of the new  
259 linear regression for reconstructing the past SST with the fossil  $\delta^{18}\text{O}_{\text{shell}}$  is a valid approach.

#### 260 4.2 Indication of seasonal variation in modern *Tridacna*

261 According to  $\delta^{18}\text{O}_{\text{YX1}}$  (-0.60 to -1.52 ‰) and  $\delta^{18}\text{O}_{\text{predicted}}$  (-0.47 to -1.57 ‰) profiles (Fig. 4b),  
262 seasonality is shown with the lowest value occurring in the first r-month (cold season) and the  
263 highest value in the fourth r-month (warm season). The difference in seasonality between  $\delta^{18}\text{O}_{\text{YX1}}$   
264 and  $\delta^{18}\text{O}_{\text{predicted}}$  is 0.18 ‰, which accounts for 19 % of  $\delta^{18}\text{O}_{\text{YX1}}$ . This situation may be due to the  
265 different growth rates and equidistance sampling mode. In each year, the analyzed *Tridacna* grew  
266 faster in warmer seasons than in colder seasons; thus, specimens under equidistance sampling mode  
267 have more samples in the warm seasons. Fewer points in the cold seasons decrease the values and  
268 lead to a lower  $\delta^{18}\text{O}_{\text{shell}}$  in the first r-month, but the higher number of points make  $\delta^{18}\text{O}_{\text{shell}}$  close to  
269  $\delta^{18}\text{O}_{\text{predicted}}$  in the warm seasons (nearly identical in the fourth r-month). Moreover, throughout the  
270 life of the analyzed *Tridacna*, the  $\delta^{18}\text{O}_{\text{shell}}$  yearly amplitude increasingly approaches to the actual  
271  $\delta^{18}\text{O}_{\text{predicted}}$  when using a greater number of points (fast growth rate) before reaching maturity. After  
272 the *Tridacna* reached maturity, the fewer points obtained under equidistance mode in a year yielded  
273 a lower amplitude. This can explain the minor discrepancy between  $\delta^{18}\text{O}_{\text{shell}}$  and  $\delta^{18}\text{O}_{\text{predicted}}$ . As a  
274 result,  $\delta^{18}\text{O}_{\text{shell}}$  slightly reduced the actual seasonal variation. However, the correlation between  
275 them is high ( $r = 0.81$ ,  $n = 77$ ), and the mean  $\delta^{18}\text{O}_{\text{YX1}}$  (-1.15 ‰) and mean  $\delta^{18}\text{O}_{\text{predicted}}$  (-1.14 ‰)  
276 values are similar. Therefore,  $\delta^{18}\text{O}_{\text{shell}}$  can also be used to estimate the actual seasonal variation, with  
277 caution regarding the slightly reduced variation.

#### 278 4.3 Reconstructed climate with fossil *Tridacna* A5 $\delta^{18}\text{O}$ evidence

279 The fossil *Tridacna* lived 3700 years ago during early Meghalayan. The 40  $\delta^{18}\text{O}_{\text{A5}}$  cycles  
280 reveal that *Tridacna* A5 had probably lived for at least 40 years. After calculating data into r-monthly  
281 average profiles, the extreme seasonal variation effects were minimized. The mean  $\delta^{18}\text{O}_{\text{A5}}$  is -  
282 1.34 ‰, with a minimum and maximum of -1.66 and 0.66 ‰, respectively (Fig. 4c). Contrasting  
283 with the mean value of YX1 (-1.15 ‰), the lower  $\delta^{18}\text{O}_{\text{A5}}$  mean value may have reflected the higher  
284 temperature that *Tridacna* A5 lived in during the warmer season. To translate into SST (without  
285 considering the SSS changes), the temperature was estimated to be roughly 0.84°C higher than the  
286 present. This agrees with other lines of evidence that suggest a higher temperature during that period  
287 (Ouyang et al., 2016), considered to be part of the Holocene megathermal in China (Shi et al., 1992).

288 The average r-monthly seasonal range of this period (1 ‰) is similar to that yielded from  
289 YX1 (0.92 ‰). The SD of  $\delta^{18}\text{O}_{\text{A5}}$  (0.38 ‰,  $n=281$ ) and  $\delta^{18}\text{O}_{\text{YX1}}$  (0.35 ‰,  $n=77$ ) are also similar.  
290 These results show similar climate change 3700 years ago and in the present. However, the life of  
291 *Tridacna* YX1 (11 years) was much shorter than the fossil *Tridacna* (which lived for at least 40

292 years), and YX1's location is in the southern of A5's; thus modern observation data from the North  
293 Reef were used to do the climatic comparison. After translating  $\delta^{18}\text{O}_{\text{A5}}$  into SST (Fig. 5), the  
294 reconstructed SST shows an average maximum and minimum of 30 °C and 25.61 °C, respectively,  
295 with a seasonal variation of 4.39 °C (Fig. 4e). Comparatively, the r-monthly average range of  
296 modern observation is 29.33 to 23.99 °C (from 1982 to 2017), with a seasonal variation of 5.34 °C  
297 (Fig. 4e). The warmer climate in the past, associated with seasonality variance, is about 0.95 °C  
298 lower. Considering the seasonality discrepancy between  $\delta^{18}\text{O}_{\text{shell}}$  and  $\delta^{18}\text{O}_{\text{predicted}}$ , the  $\delta^{18}\text{O}_{\text{shell}}$  has a  
299 19 % lower seasonal variation than  $\delta^{18}\text{O}_{\text{predicted}}$ . Therefore, the actual seasonal variation of A5  
300 (roughly 5.23 °C) is still below present seasonality.

301 In addition, the discrepancy between mean  $\delta^{18}\text{O}_{\text{A5}}$  and mean  $\delta^{18}\text{O}_{\text{YX1}}$  is 0.19 ‰; the lower  
302 mean  $\delta^{18}\text{O}_{\text{A5}}$  is because of more r-months in lower values. This reveals a possible prolonged high-  
303 temperature period 3700 years ago: warm seasons may have been longer, while cold seasons may  
304 have been shorter. This agrees with a comparison between 3700 years ago (3722 to 3623 BP) and  
305 the past century (1918 to 2017), which indicates *Tridacna* A5 lived in more insolation. This occurs  
306 from the second to fifth r-month (warm seasons); however, less insolation occurs in the rest of the  
307 months (Fig. 4d). Thus, the prolonged high-temperature in the past might be attributed to more  
308 insolation. In addition, although a higher sampling density obtained in the warm seasons enlarges  
309 the high-temperature period (from the second to sixth r-month), a cold-to-warm transition could still  
310 be recognized in A5 and YX1  $\delta^{18}\text{O}$  profiles (Fig. 4c). Comparison of each r-monthly value with the  
311 average value shows that between the first and second r-month had a larger deviation with a greater  
312 slope 3700 years ago. This illustrates a fast transition between cold and warm seasons 3700 years  
313 ago. As  $\delta^{18}\text{O}_{\text{predicted}}$  has stronger seasonal variation than  $\delta^{18}\text{O}_{\text{shell}}$ , the slope should be sharper, which  
314 means more significant actual seasonal transition.

315 Overall, the climate around 3700 years ago had slightly lower seasonality than the present,  
316 and the transition between cold and warm seasons was starker.

#### 317 4.4 Climate variation comparison between 3700 years ago and present

318 A comparison was performed between the modern instrumental observations (from 1982 to  
319 2017) in the North Reef and the reconstructed SST anomalies of *Tridacna* A5. The r-monthly  
320 resolution data were first compared, obtained by subtracting the r-monthly SST with the mean value  
321 of each r-month. In terms of long-term climatic variation, the SST anomalies are markedly different  
322 between the 36-year modern instrumental data and the 40-year reconstructed data (Fig. 6a). The  
323 SST anomalies (3700 years ago) have sharper peaks and a greater amplitude than in those of recent  
324 years, and the SD in the past is much larger (0.68 °C) than in the present (0.42 °C), suggesting more  
325 severe climate conditions in the past. However, the deviation should be noted alongside the different  
326 growth rates during *Tridacna*'s lifespan and in equidistant sampling mode. For example, *Tridacna*  
327 may have different annual growth rates, hence an r-monthly value may not represent the  
328 corresponding actual r-monthly value under equidistant sampling mode. In this respect, the r-annual

329 SST anomalies are estimated to reduce the deviation (Fig. 6b). The SD of modern observation SST  
330 anomalies is 0.30 °C, and the SD of reconstructed SST anomalies is 0.41 °C. This illustrates that  
331 the modern-to-past ratios of the r-monthly resolutions or r-annual resolutions are almost the same  
332 (0.65 and 0.73, respectively); thus the SD of r-monthly SST anomalies of *Tridacna* is likely a reliable  
333 measure. As a result, the enhanced climate variability 3700 years ago probably indicates increased  
334 ENSO-related variability in this region. This conclusion contradicts data from samples (deep-sea  
335 sediments and fossil mollusk shells) collected in the eastern tropical Pacific at the same time period  
336 (Koutavas et al., 2012, Carré et al., 2014). More data should be analyzed from long, successive time  
337 periods to understand more about the dynamics of ENSO on a large scale.

#### 338 4.5 ENSO activity recorded by *Tridacna* $\delta^{18}O$

339 As ENSO is the strongest contributor to global interannual climate variation, a better  
340 understanding of its fundamental properties will allow us to better unravel past climate change  
341 episodes and to make more accurate predictions for the future. Interannual climate changes in the  
342 Xisha Islands were likely dominated by ENSO activity. The local accumulated positive percentage  
343 of monthly SST anomalies threshold respond to 76.47 % El Niño and 79.41 % La Niña events in  
344 Niño 3.4 region (Liu et al., 2016). Previous studies demonstrate that marine biogenic carbonate-  
345 based SST reconstructions in the northern South China Sea likely responded to ENSO activity (Sun  
346 et al., 2005; Yan et al., 2017). Warm (cold) SST anomalies are related to El Niño (La Niña) events.  
347 Coral has one of the earliest records revealing ENSO events (Peng et al., 2003; Sun et al., 2005; Wei  
348 et al., 2007), yet there are still some technical limitations in using coral, such as those concerning  
349 post-depositional diagenetic alteration between aragonite and calcite (McGregor and Gagan, 2003).  
350 Analyses of *Tridacna* species are performed to overcome this limitation by taking advantage of their  
351 denser shells, lack of diagenetic alteration, and oxygen isotopic equilibrium with seawater. Recently,  
352 Yan et al. (2014) proved that *Tridacna* species in the Xisha Islands respond to ENSO activity, and  
353 then used fossil *Tridacna*  $\delta^{18}O$  in Dongdao Island (part of the Xisha Islands) to reconstruct ENSO  
354 variability around 2000 years ago (Yan et al., 2017).

355 To acquire more precise ENSO reconstructions, modern observation data were analyzed and  
356 compared with the SST in Niño 1 + 2 region. The SST anomaly series were calculated by subtracting  
357 the r-monthly mean values. The spectral analyses were performed to test periodicity among all SST  
358 anomalies (Fig. 7), which indicate a spectral peak of 3 to 7 years. According to the SST series, the  
359 North Reef SST has a 3 r-month time lag behind the Niño 1 + 2 SST (Fig. 8a), and thus 3-r-months  
360 of the North Reef SST were brought forward to eliminate the lag. To reconstruct the occurrence of  
361 ENSO in the North Reef, 3-7 years of bandpass filtering was performed on the SST anomalies,  
362 which yielded North Reef ENSO activity mostly consistent with the Niño 1 + 2 SST anomalies (Fig.  
363 8c). A threshold value was calculated under  $1\sigma$  SST anomalies for moderate El Niño/La Niña events.  
364 A total of seven El Niño and ten La Niña events occurred in the past 36 years. In other words, El  
365 Niño/La Niña events occurred successively at a 5.14-year frequency in the North Reef.

366 Spectral analysis revealed that  $\delta^{18}\text{O}_{\text{A5}}$  anomalies also have a 3 to 7 years period (Fig. 7c). As  
367 discussed above, the *Tridacna*  $\delta^{18}\text{O}$  values are mainly dominated by SST in the Xisha Islands, and  
368  $1\text{‰ } \delta^{18}\text{O}_{\text{shell}}$  is roughly equal to  $4.41\text{ }^{\circ}\text{C}$  of SST.  $\delta^{18}\text{O}_{\text{A5}}$  anomalies were transformed into the North  
369 Reef SST<sub>A5</sub> anomalies (Fig. 9b). After the 3–7 years of bandpass filtering of the North Reef SST<sub>A5</sub>  
370 anomalies, six El Niño and five La Niña events were estimated to occur over 40 years with  $1\sigma$  SST<sub>A5</sub>  
371 anomalies threshold (Fig. 9c), giving a 6.67 and 8-year frequency, respectively. The ENSO  
372 frequency is reduced when compared with modern observation data. The lower frequency is  
373 supported in ENSO reconstructions back to 7 ka, which suggest a notable reduction of ENSO  
374 between 5 and 3 ka (Liu et al., 2013; McGregor et al., 2013; Tudhope et al., 2001; Emile-Geay et  
375 al., 2016). However, implications drawn from a mere 40-year long *Tridacna*  $\delta^{18}\text{O}$  record are likely  
376 inconclusive. A collection of more similar-aged *Tridacna* is needed to develop a more continuous  
377 climate and ENSO activity record in Holocene.

#### 378 4.6 Extreme winter El Niño records in fossil *Tridacna* $\delta^{18}\text{O}$ values

379 In recent decades, extreme El Niño has brought about many climatic disasters, such as  
380 catastrophic flooding, bushfire and drought (Ramírez and Briones, 2017; Staupe-Delgado et al.,  
381 2018; Yu et al., 2018; Yu et al., 2019). With global warming persisting, the question of whether high  
382 temperatures are related to extreme El Niño events is still controversial. Therefore, records of  
383 extreme El Niño events in past warm periods are important. Here, the winter SST is used to estimate  
384 extreme El Niño events. Winters in the northern South China Sea are very dry, and the SSS variation  
385 caused by rainfall is small. Thus, the SST determined from  $\delta^{18}\text{O}_{\text{shell}}$  should be close to the actual  
386 value. The SST calculated by  $\delta^{18}\text{O}_{\text{YX1}}$  reveals a warmer winter in 1998, corresponding to a stronger  
387 El Niño that year. A comparison between the reconstructed SST (calculated with  $\delta^{18}\text{O}_{\text{A5}}$ ) and modern  
388 observation data from the North Reef (Fig. 5), suggested that the average winter SST 3700 years  
389 ago was  $25.62\text{ }^{\circ}\text{C}$ . There are six distinctly high SST within the 40 years (gray fields in Fig. 5), with  
390 anomalies ranging from  $0.73$  to  $2.00\text{ }^{\circ}\text{C}$ . As for the SST of modern observation (from 1982 to 2017),  
391 the average of winter SST is  $23.99\text{ }^{\circ}\text{C}$ , and three anomalously warm temperatures vary from  $0.60$  to  
392  $1.38\text{ }^{\circ}\text{C}$ . It seems that extreme El Niño winter events were very frequent in this past warm period.  
393 However, this analysis still provides low confidence in answering this controversial question about  
394 the relationship between El Niño events and warm climate; more *Tridacna* in the past warm period  
395 should be analyzed in future work. Nevertheless, our results still put forward high-resolution data  
396 that make a contribution to future work on how El Niño events occur in warm periods.

397

## 398 5 Conclusions

399 The  $\delta^{18}\text{O}$  derived from *Tridacna* provide high-resolution data, useful to unravel climatic  
400 variability and ENSO activity. In the Xisha Islands of the northern South China Sea, the  $\delta^{18}\text{O}_{\text{shell}}$  of  
401 modern *Tridacna gigas* can serve as a proxy for SST, while SSS has a minor effect on  $\delta^{18}\text{O}_{\text{shell}}$ .  
402 Thus, a rough  $\delta^{18}\text{O}$ –SST linear regression is established:  $\text{SST} (^{\circ}\text{C}) = 22.69 - 4.41 \times \delta^{18}\text{O}_{\text{shell}}$ . Another

403 *Tridacna squamosa* A5, which lived 3700 years ago, reveals 40 clearly dark/bright line couples  
404 consistent with  $\delta^{18}\text{O}_{\text{shell}}$  profiles. Reconstructed SST implies a warmer climate 3700 years ago,  
405 0.84 °C higher than the present. The seasonal variation slightly decreased and the transition among  
406 cold to warm seasons was faster. The combinations of SST anomalies reconstructed at r-monthly/r-  
407 annual resolution suggest enhanced ENSO-related variability during this past warm period. In  
408 addition, the frequency of ENSO activity was less 3700 years ago than during the recent 36-years  
409 modern observation. El Niño/La Niña events occurred alternatively at a frequency of every 6.67/8  
410 years in the past, compared to every 5.14 years in recent decades. Extreme El Niño winters have  
411 been recorded by a fossil *Tridacna* with increased numbers and intense variations. Our results imply  
412 an unstable climate 3700 years ago, although more data are still needed to support this hypothesis.  
413

## 414 **Author contributions**

415 X. M. S., H. Y., and Y. H. designed the research and experiments; H. Y. collected the samples;  
416 H. C., and Y. H. performed stable isotope measurements. H. Y. and Y. H. did the data analyses. Y.  
417 H. wrote the manuscript, with the help of all co-authors.  
418

## 419 **Competing interests**

420 The authors declare that they have no conflict of interest.  
421

## 422 **Data and materials availability**

423 All data needed to evaluate the conclusions in the paper are presented in the paper. Additional  
424 data related to this paper may be requested from the authors. Correspondence and requests for  
425 materials should be addressed to X. M. S. (eessxm@mail.sysu.edu.cn) and H. Y.  
426 ([yanhong@ieecas.cn](mailto:yanhong@ieecas.cn)).  
427

## 428 **Acknowledgments**

429 This work is supported by the projects from the National Key R&D Program of China  
430 (2018YFA0702605), the National 13<sup>th</sup> Five Year Plan Project (DY135-R2-1-01, DY135-C1-1-06),  
431 National Nature Science Foundation of China (41876038, 41877399, 91128101, 41888101), State  
432 Key Laboratory for Mineral Deposits Research in Nanjing University (no. 20–15–07), Chinese  
433 Academy of Sciences (QYZDB-SSW-DQC001), and Qingdao National Laboratory for Marine  
434 Science and Technology of China (QNL2016ORP0202). We are grateful to Yu Fu, Yang Lu,  
435 Jiaoyang Ruan, Chengcheng Liu, Tianjian Yang, and Jun Gu for their support in preparing the  
436 manuscript. Youfeng Ning, Hanying Li, Pengfei Duan, and Jingyao Zhao are thanked for their  
437 technical support in drilling and analyses at Xi'an Jiaotong University.



439 **References**

- 440 Agbaje, O. B. A., Wirth, R., Morales, L. F. G., Shirai, K., Kosnik, M., Watanabe, T. and Jacob, D. E.:  
 441 Subject Category : Subject Areas : Architecture of crossed-lamellar bivalve shells : the southern giant  
 442 clam ( *Tridacna derasa* , Röding, 1798), R. Soc. Open Sci., 1–15,  
 443 doi:https://doi.org/10.1098/rsos.170622, 2017.
- 444 Aharon, P.: 140,000-yr isotope climatic record from raised coral reefs in New Guinea, *Nature*, 304(5928),  
 445 720–723, doi:10.1038/304720a0, 1983.
- 446 Aharon, P.: Recorders of reef environment histories: stable isotopes in corals, giant clams, and calcareous  
 447 algae, *Coral Reefs*, 10(2), 71–90, doi:10.1007/BF00571826, 1991.
- 448 Aharon, P. and Chappell, J.: Oxygen isotopes, sea level changes and the temperature history of a coral  
 449 reef environment in New Guinea over the last 105 years, *Palaeogeogr. Palaeoclimatol. Palaeoecol.*,  
 450 56(3–4), 337–379, doi:10.1016/0031-0182(86)90101-X, 1986.
- 451 Arias-Ruiz, C., Elliot, M., Bézous, A., Pedoja, K., Husson, L., Cahyarini, S. Y., Cariou, E., Michel, E.,  
 452 La, C. and Manssouri, F.: Geochemical fingerprints of climate variation and the extreme La Niña  
 453 2010–11 as recorded in a *Tridacna squamosa* shell from Sulawesi, Indonesia, *Palaeogeogr.*  
 454 *Palaeoclimatol. Palaeoecol.*, 487, 216–228, doi:10.1016/j.palaeo.2017.08.037, 2017.
- 455 Ayling, B. F., Chappell, J., Gagan, M. K. and McCulloch, M. T.: ENSO variability during MIS 11 (424–  
 456 374 ka) from *Tridacna gigas* at Huon Peninsula, Papua New Guinea, *Earth Planet. Sci. Lett.*, 431,  
 457 236–246, doi:10.1016/j.epsl.2015.09.037, 2015.
- 458 Batenburg, S. J., Reichert, G. J., Jilbert, T., Janse, M., Wesselingh, F. P. and Renema, W.: Interannual  
 459 climate variability in the Miocene: High resolution trace element and stable isotope ratios in giant  
 460 clams, *Palaeogeogr. Palaeoclimatol. Palaeoecol.*, 306(1–2), 75–81, doi:10.1016/j.palaeo.2011.03.031,  
 461 2011.
- 462 Cane, M. A.: The evolution of El Niño, past and future, *Earth Planet. Sci. Lett.*, 230(3–4), 227–240,  
 463 doi:10.1016/j.epsl.2004.12.003, 2005.
- 464 Carré, M., Sachs, J. P., Purca, S., Schauer, A. J., Braconnot, P., Falcón, R. A., Julien, M. and Lavallée,  
 465 D.: Holocene history of ENSO variance and asymmetry in the eastern tropical Pacific,  
 466 *Paleoceanography*, 345(6200), 1045–1048, doi:10.1126/science.1252220, 2014.
- 467 Cobb, K. M., Westphal, N., Sayani, H. R., Watson, J. T., Lorenzo, E. Di, Cheng, H., Edwards, R. L. and  
 468 Charles, C. D.: Highly Variable El Niño–Southern Oscillation Throughout the Holocene, *Science*  
 469 (80-. ), 339, 67–70, doi:10.1126/science.1228246, 2014.
- 470 Duprey, N., Galipaud, J. C., Cabioch, G. and Lazareth, C. E.: Isotopic records from archeological giant  
 471 clams reveal a variable climate during the southwestern Pacific colonization ca. 3.0ka BP,  
 472 *Palaeogeogr. Palaeoclimatol. Palaeoecol.*, 404, 97–108, doi:10.1016/j.palaeo.2014.04.002, 2014.
- 473 Elliot, M., Welsh, K., Chilcott, C., McCulloch, M., Chappell, J. and Ayling, B.: Profiles of trace elements  
 474 and stable isotopes derived from giant long-lived *Tridacna gigas* bivalves: Potential applications in  
 475 paleoclimate studies, *Palaeogeogr. Palaeoclimatol. Palaeoecol.*, 280(1–2), 132–142,  
 476 doi:10.1016/j.palaeo.2009.06.007, 2009.

477 Emile-Geay, J., Cobb, K. M., Carre, M., Braconnot, P., Leloup, J., Zhou, Y., Harrison, S. P., Corrège, T.,  
478 McGregor, H. V., Collins, M., Driscoll, R., Elliot, M., Schneider, B. and Tudhope, A.: Links between  
479 tropical Pacific seasonal, interannual and orbital variability during the Holocene, *Nat. Geosci.*, 9(2),  
480 168–173, doi:10.1038/ngeo2608, 2016.

481 Gannon, M. E., Pérez-Huerta, A., Aharon, P. and Street, S. C.: A biomineralization study of the Indo-  
482 Pacific giant clam *Tridacna gigas*, *Coral Reefs*, 36(2), 503–517, doi:10.1007/s00338-016-1538-5,  
483 2017.

484 Hong, ashi, Hong, ying, Wang, qingchun and Ke, jingtang: Distributive characteristics of O isotope of  
485 the northeastern South China Sea in the summer of 1994, *Trop. Oceanol.*, 16(2), 82–90, available  
486 from: <http://kns.cnki.net/kns/detail/detail.aspx?FileName=RDHY199702006&DbName=CJFQ1997,>  
487 1997.

488 Koutavas, A. and Joanides, S.: El Niño – Southern Oscillation extrema in the Holocene and Last Glacial  
489 Maximum, *Paleoceanography*, 27(October), 1–15, doi:10.1029/2012PA002378, 2012.

490 Laskar, J., Robutel, P., Joutel, F., Gastineau, M., Correia, A. C. M. and Levrard, B.: A long-term  
491 numerical solution for the insolation quantities of the Earth, *Astron. Astrophys.*, 428(1), 261–285,  
492 doi:10.1051/0004-6361:20041335, 2004.

493 Liu, C., Yan, H., Fei, H., Ma, X., Zhang, W. and Shi, G.: Journal of Asian Earth Sciences Temperature  
494 seasonality and ENSO variability in the northern South China Sea during the Medieval Climate  
495 Anomaly interval derived from the Sr / Ca ratios of *Tridacna* shell, *J. Asian Earth Sci.*, 180(June), 1-  
496 9, doi:10.1016/j.jseaes.2019.103880, 2019.

497 Liu, C., Zhang, W. and Yan, H.: Relationship between El Niño-Southern Oscillation events and regional  
498 sea surface temperature anomalies around the Xisha Islands, South China Sea, *J. Earth Environ.*, 1(1),  
499 1188–1197, doi:10.7515/JEE201702007, 2016.

500 Liu, C., Yan, H., Fei, H., Ma, X., Zhang, W. and Shi, G.: Journal of Asian Earth Sciences Temperature  
501 seasonality and ENSO variability in the northern South China Sea during the Medieval Climate  
502 Anomaly interval derived from the Sr / Ca ratios of *Tridacna* shell, *J. Asian Earth Sci.*, 180(June), 1–  
503 9, doi:10.1016/j.jseaes.2019.103880, 2019.

504 Liu, J., Li, T., Xiang, R., Chen, M., Yan, W., Chen, Z. and Liu, F.: Influence of the Kuroshio Current  
505 intrusion on Holocene environmental transformation in the South China Sea, *Holocene*, 23(6), 850–  
506 859, doi:10.1177/0959683612474481, 2013.

507 McGregor, H. V. and Gagan, M. K.: Diagenesis and geochemistry of Porites corals from Papua New  
508 Guinea: Implications for paleoclimate reconstruction, *Geochim. Cosmochim. Acta*, 67(12), 2147–  
509 2156, doi:10.1007/430\_2015\_174, 2003.

510 McGregor, H. V., Fischer, M. J., Gagan, M. K., Fink, D., Phipps, S. J., Wong, H. and Woodroffe, C. D.:  
511 A weak El Niño/Southern Oscillation with delayed seasonal growth around 4,300 years ago, *Nat.*  
512 *Geosci.*, 6(11), 949–953, doi:10.1038/ngeo1936, 2013.

513 Mitsuguchi, T., Dang, P. X., Kitagawa, H., Uchida, T. and Shibata, Y.: Coral Sr/Ca and Mg/Ca records  
514 in Con Dao Island off the Mekong Delta: Assessment of their potential for monitoring ENSO and  
515 East Asian monsoon, *Glob. Planet. Change*, 63(4), 341–352, doi:10.1016/j.gloplacha.2008.08.002,

516 2008.

517 Ourbak, T., Corrège, T., Malaizé, B., Le Cornec, F., Charlier, K. and Peypouquet, J. P.: ENSO and  
518 interdecadal climate variability over the last century documented by geochemical records of two coral  
519 cores from the South West Pacific, *Adv. Geosci.*, 6, 23–27, doi:10.5194/adgeo-6-23-2006, 2006.

520 Ouyang, T., Li, M., Zhao, X., Zhu, Z., Tian, C., Qiu, Y., Peng, X. and Hu, Q.: Sensitivity of Sediment  
521 Magnetic Records to Climate Change during Holocene for the Northern South China Sea, *Front.*  
522 *Earth Sci.*, 4(May), 1–12, doi:https://doi.org/10.3389/feart.2016.00054, 2016.

523 Pätzold, J., Heinrichs, J. P., Wolschendorf, K. and Wefer, G.: Correlation of stable oxygen isotope  
524 temperature record with light attenuation profiles in reef-dwelling *Tridacna* shells, *Coral Reefs*, 10(2),  
525 65–69, doi:10.1007/BF00571825, 1991.

526 Peng, Z., Chen, T., Nie, B., Head, M. J., He, X. and Zhou, W.: Coral  $\delta^{18}\text{O}$  records as an indicator of  
527 winter monsoon intensity in the South China Sea, *Quat. Res.*, 59(3), 258–292, doi:10.1016/S0033-  
528 5894(03)00042-5, 2003.

529 Ramírez, I. J. and Briones, F.: Understanding the El Niño Costero of 2017: The Definition Problem and  
530 Challenges of Climate Forecasting and Disaster Responses, *Int. J. Disaster Risk Sci.*, 8(4), 489–492,  
531 doi:10.1007/s13753-017-0151-8, 2017.

532 Rodbell, D. T., Seltzer, G. O., Anderson, D. M., Abbott, M. B., Enfield, D. B. and Newman, J. H.: An  
533 ~15,000-Year Record of El Niño-Driven Alluviation in Southwestern Ecuador.pdf, *Science*,  
534 283(5401), 516–520, doi:10.1126/science.283.5401.516, 1999.

535 Romanek, C. S. and Grossman, E. L.: Stable Isotope Profiles of *Tridacna* maxima as Environmental  
536 Indicators Stable Isotope Profiles of *Tridacna* maxima as Environmental Indicators, *Palaios*, 4(5),  
537 402–413, doi:10.2307/351458, 1989.

538 Schirrmacher, J., Weinelt, M., Blanz, T., Andersen, N., Salgueiro, E. and Schneider, R. R.: Multi-decadal  
539 climate variability in southern Iberia during the mid- to late-Holocene, *Clim. Past*, 15(2), 617–634,  
540 doi:10.5194/cp-15-367-2019, 2019.

541 Schöne, B. R. and Fiebig, J.: Seasonality in the North Sea during the Allerød and Late Medieval Climate  
542 Optimum using bivalve sclerochronology, *Int. J. Earth Sci.*, 98(1), 83–98, doi:10.1007/s00531-008-  
543 0363-7, 2009.

544 Schöne, B. R., Fiebig, J., Pfeiffer, M., Gleß, R., Hickson, J., Johnson, A. L. A., Dreyer, W. and Oschmann,  
545 W.: Climate records from a bivalved Methuselah (*Arctica islandica*, Mollusca; Iceland), *Palaeogeogr.*  
546 *Palaeoclimatol. Palaeoecol.*, 228(1–2), 130–148, doi:10.1016/j.palaeo.2005.03.049, 2005.

547 Schöne, B. R., Fiebig, J., Pfeiffer, M., Gleß, R., Hickson, J., Johnson, A. L. A., Dreyer, W. and Oschmann,  
548 W.: Climate records from a bivalved Methuselah (*Arctica islandica*, Mollusca; Iceland), *Palaeogeogr.*  
549 *Palaeoclimatol. Palaeoecol.*, 228(1–2), 130–148, doi:10.1016/j.palaeo.2005.03.049, 2005.

550 Scuderi, L. A., Yang, X., Ascoli, S. E. and Li, H.: The 4.2 ka BP Event in northeastern China : a geospatial  
551 perspective, *Clim. Past*, 15(1), 367–375, doi:10.5194/cp-15-367-2019, 2019.

552 Shi, Y., Kong, Z., Wang, S., Tang, L., Wang, F., Yao, T., Zhao, X., Zhang, P. and Shi, S.: The Climatic  
553 Fluctuation and Important Events of Holocene Megathermal in China, *Sci. CHINA*, 37(3), 353–365 ,  
554 Available from: <http://ir.nigpas.ac.cn/handle/332004/4853>, 1994.

555 Staupe-Delgado, R., Kruke, B. I., Ross, R. J. and Glantz, M. H.: Preparedness for slow-onset  
556 environmental disasters: Drawing lessons from three decades of El Niño impacts, *Sustain. Dev.*, 26(6),  
557 553–563, doi:10.1002/sd.1719, 2018.

558 Su, R., Sun, D., Bloemendal, J. and Zhu, Z.: Temporal and spatial variability of the oxygen isotopic  
559 composition of massive corals from the South China Sea: Influence of the Asian monsoon,  
560 *Palaeogeogr. Palaeoclimatol. Palaeoecol.*, 240(3–4), 630–648, doi:10.1016/j.palaeo.2006.03.012,  
561 2006.

562 Sun, D., Gagan, M. K., Cheng, H., Scott-Gagan, H., Dykoski, C. A., Edwards, R. L. and Su, R.: Seasonal  
563 and interannual variability of the Mid-Holocene East Asian monsoon in coral  $\delta^{18}\text{O}$  records from the  
564 South China Sea, *Earth Planet. Sci. Lett.*, 237(1–2), 69–84, doi:10.1016/j.epsl.2005.06.022, 2005.

565 Thompson, L. G., Davis, M. E., Lin, P., Henderson, K. A., Bolzan, J. F. and Liu, K.: Late glacial stage  
566 and Holocene tropical ice core records from Huascarán, Peru, *Science*, 269(5220), 46–50,  
567 doi:10.1126/science.269.5220.46, 1995.

568 Toth, L. T. and Aronson, R. B.: The 4.2 ka event, ENSO, and coral reef development, *Clim. Past*, 15, 105–  
569 119, doi:10.5194/cp-15-105-2019, 2019.

570 Tudhope, A. W., Chilcott, C. P., McCulloch, M. T., Cook, E. R. and coauthors: Variability in the El  
571 Niño-Southern Oscillation through a glacial-interglacial cycle, *Science*, 291, 1511–1517,  
572 doi:10.1126/science.1057969, 2001.

573 Wanamaker, A. D., Kreutz, K. J., Schöne, B. R. and Introne, D. S.: Gulf of Maine shells reveal changes  
574 in seawater temperature seasonality during the Medieval Climate Anomaly and the Little Ice Age,  
575 *Palaeogeogr. Palaeoclimatol. Palaeoecol.*, 302(1), 43–51, doi:10.1016/j.palaeo.2010.06.005, 2011.

576 Watanabe, T., Oba, T. and Dee, V.: Daily reconstruction of water temperature from oxygen isotopic  
577 ratios of a modern *Tridacna* shell using a freezing microtome sampling technique was recorded  
578 monthly to seasonal sea surface to reconstruct using Jones maturity of *Tridacna maxima* resolution f,  
579 *J. Geophys. Res.*, 104(C9), 20667–20674, doi:10.1029/1999JC900097, 1999.

580 Watanabe, T., Suzuki, A., Kawahata, H., Kan, H. and Ogawa, S.: A 60-year isotopic record from a mid-  
581 Holocene fossil giant clam (*Tridacna gigas*) in the Ryukyu Islands: Physiological and paleoclimatic  
582 implications, *Palaeogeogr. Palaeoclimatol. Palaeoecol.*, 212(3–4), 343–354,  
583 doi:10.1016/j.palaeo.2004.07.001, 2004.

584 Wei, G., Deng, W., Yu, K., Li, X. H., Sun, W. and Zhao, J. X.: Sea surface temperature records in the  
585 northern South China Sea from mid-Holocene coral Sr/Ca ratios, *Paleoceanography*, 22(3), 1–13,  
586 doi:10.1029/2006PA001270, 2007.

587 Welsh, K., Elliot, M., Tudhope, A., Ayling, B. and Chappell, J.: Giant bivalves (*Tridacna gigas*) as  
588 recorders of ENSO variability, *Earth Planet. Sci. Lett.*, 307(3–4), 266–270,  
589 doi:10.1016/j.epsl.2011.05.032, 2011.

590 Woodroffe, C. D., Beech, M. R. and Gagan, M. K.: Mid-late Holocene El Niño variability in the  
591 equatorial Pacific from coral microatolls, *Geophys. Res. Lett.*, 30(7), 1–4,  
592 doi:10.1029/2002GL015868, 2003.

593 Yamanashi, J., Takayanagi, H., Isaji, A., Asami, R. and Iryu, Y.: Carbon and oxygen isotope records

594 from *Tridacna derasa* shells: Toward establishing a reliable proxy for sea surface environments,  
595 PLoS One, 11(6), doi:10.1371/journal.pone.0157659, 2016.

596 Yan, H., Sun, L., Liu, X. and Qiu, S.: Relationship between ENSO events and regional climate anomalies  
597 around the Xisha Islands during the last 50 years, J. Trop. Oceanogr., 29(5), 29–35,  
598 doi:https://doi.org/10.1007/s13131-014-0399-4, 2010.

599 Yan, H., Sun, L., Oppo, D. W., Wang, Y., Liu, Z., Xie, Z., Liu, X. and Cheng, W.: South China Sea  
600 hydrological changes and Pacific Walker Circulation variations over the last millennium, Nat.  
601 Commun., 2(1), 2018, doi:10.1038/ncomms1297, 2011.

602 Yan, H., Shao, D., Wang, Y. and Sun, L.: Sr/Ca profile of long-lived *Tridacna gigas* bivalves from South  
603 China Sea: A new high-resolution SST proxy, Geochim. Cosmochim. Acta, 112, 52–65,  
604 doi:10.1016/j.gca.2013.03.007, 2013.

605 Yan, H., Wang, Y. and Sun, L.: High resolution oxygen isotope and grayscale records of a medieval  
606 fossil giant clam (*Tridacna gigas*) in the South China Sea: Physiological and paleoclimatic  
607 implications, Acta Oceanol. Sin., 33(8), 18–25, doi:10.1007/s13131-014-0399-4, 2014.

608 Yan, H., Liu, C., Zhang, W., Li, M., Zheng, X., Wei, G., Xie, L., Deng, W. and Sun, L.: ENSO variability  
609 around 2000 years ago recorded by *Tridacna gigas*  $\delta^{18}\text{O}$  from the South China Sea, Quat. Int., 452,  
610 148–154, doi:10.1016/j.quaint.2016.05.011, 2017.

611 Yang, Y., Xiang, R., Liu, J. and Tang, L.: Inconsistent sea surface temperature and salinity changing  
612 trend in the northern South China Sea since 7.0 ka BP, J. Asian Earth Sci., 171, 178–186,  
613 doi:10.1016/j.jseaes.2018.05.033, 2019.

614 Yu, J., Qi, M., Sun, Q. and Tao, L.: Statistical characteristics of summer extreme rainfall over eastern  
615 China and its relation with El Niño, J. Nanjing Inst. Meteorol., 41(1), 77–84 [online] Available from:  
616 http://lib.cqvip.com/qk/91555A/201801/7000486505.html, 2018.

617 Yu, K. F., Zhao, J. X., Wei, G. J., Cheng, X. R. and Wang, P. X.: Mid-late Holocene monsoon climate  
618 retrieved from seasonal Sr/Ca and  $\delta^{18}\text{O}$  records of *Porites lutea* corals at Leizhou Peninsula, northern  
619 coast of South China Sea, Glob. Planet. Change, 47(2-4 SPEC. ISS.), 301–316,  
620 doi:10.1016/j.gloplacha.2004.10.018, 2005a.

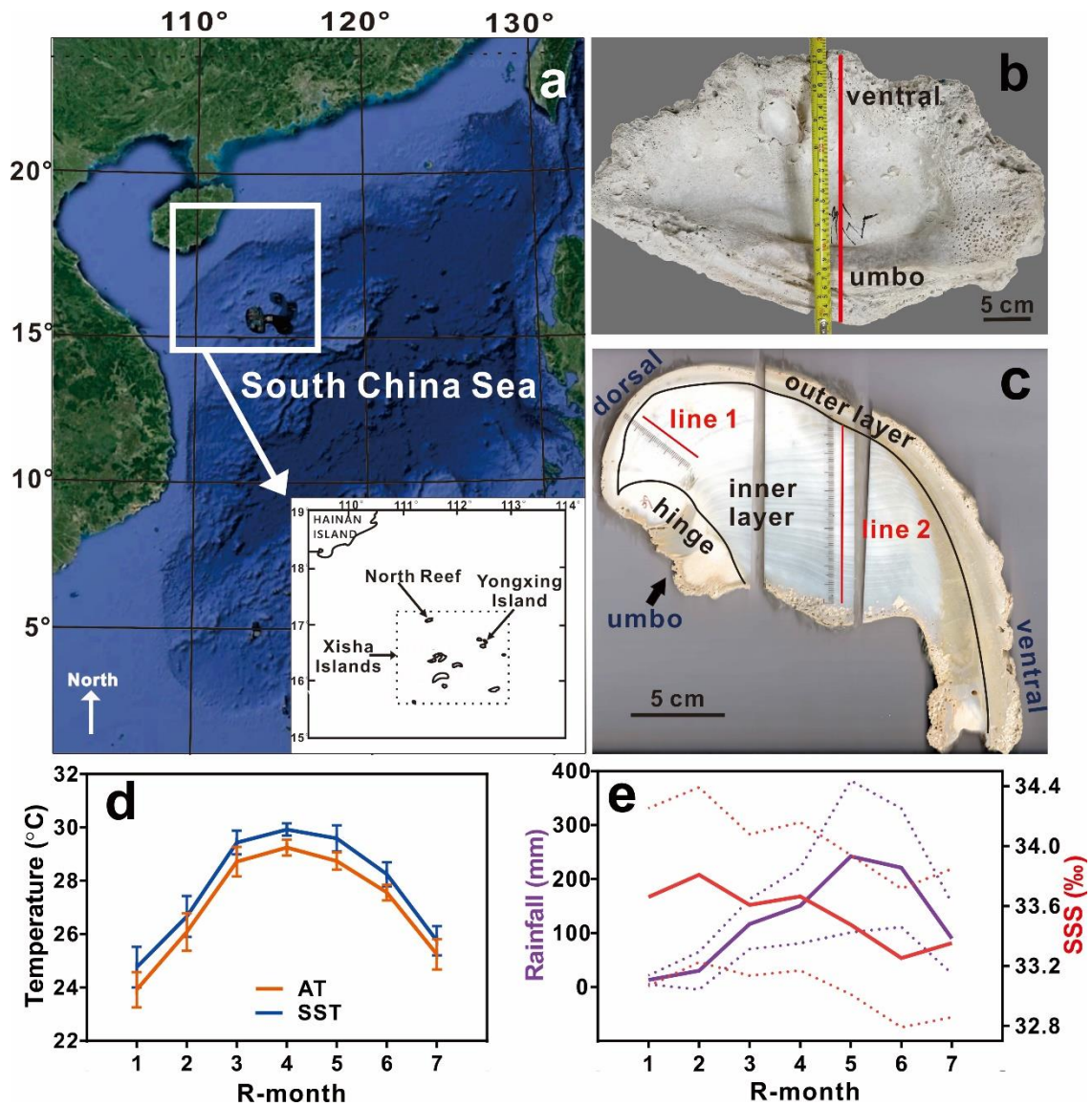
621 Yu, K. F., Zhao, J. X., Wei, G. J., Cheng, X. R., Chen, T. G., Felis, T., Wang, P. X. and Liu, T. S.:  $\delta^{18}\text{O}$ ,  
622 Sr/Ca and Mg/Ca records of *Porites lutea* corals from Leizhou Peninsula, northern South China Sea,  
623 and their applicability as paleoclimatic indicators, Palaeogeogr. Palaeoclimatol. Palaeoecol., 218(1–  
624 2), 57–73, doi:10.1016/j.palaeo.2004.12.003, 2005b.

625 Yu, X., Wang, Z., Zhang, H. and Zhao, S.: Impacts of different types and intensities of El Niño events  
626 on winter aerosols over China, Sci. Total Environ., 655, 766–780,  
627 doi:10.1016/j.scitotenv.2018.11.090, 2019.

628 Zhang, H., Cheng, H., Cai, Y., Spötl, C., Kathayat, G. and Sinha, A.: Hydroclimatic variations in  
629 southeastern China during the 4.2 ka event reflected by stalagmite records, Clim. Past, 14(11), 1805–  
630 1817, doi:10.5194/cp-14-1805-2018, 2018.

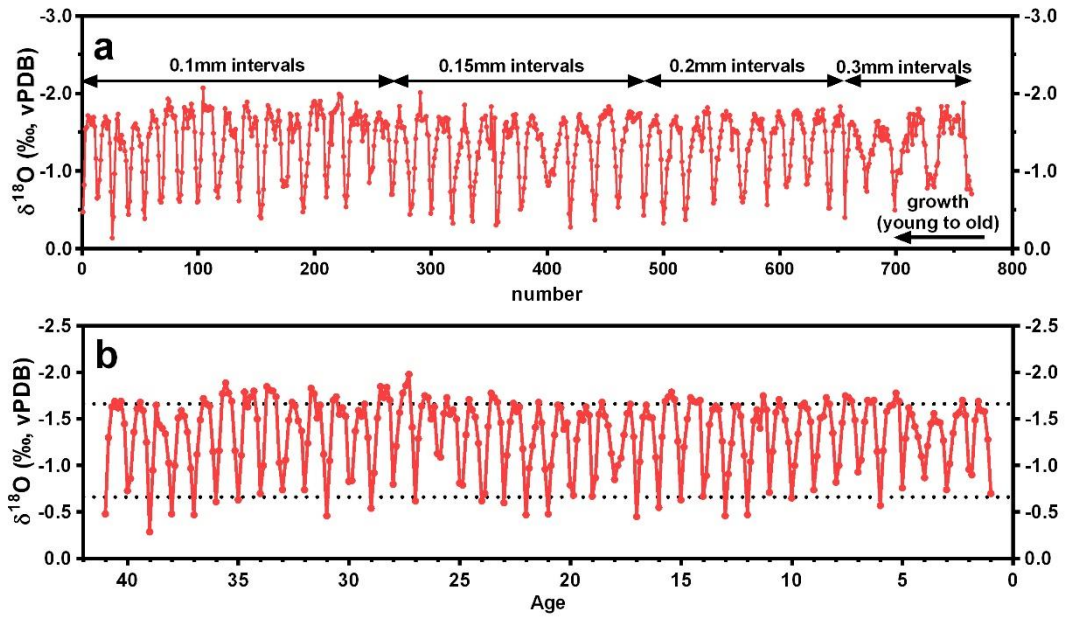
631

632 **Figures**



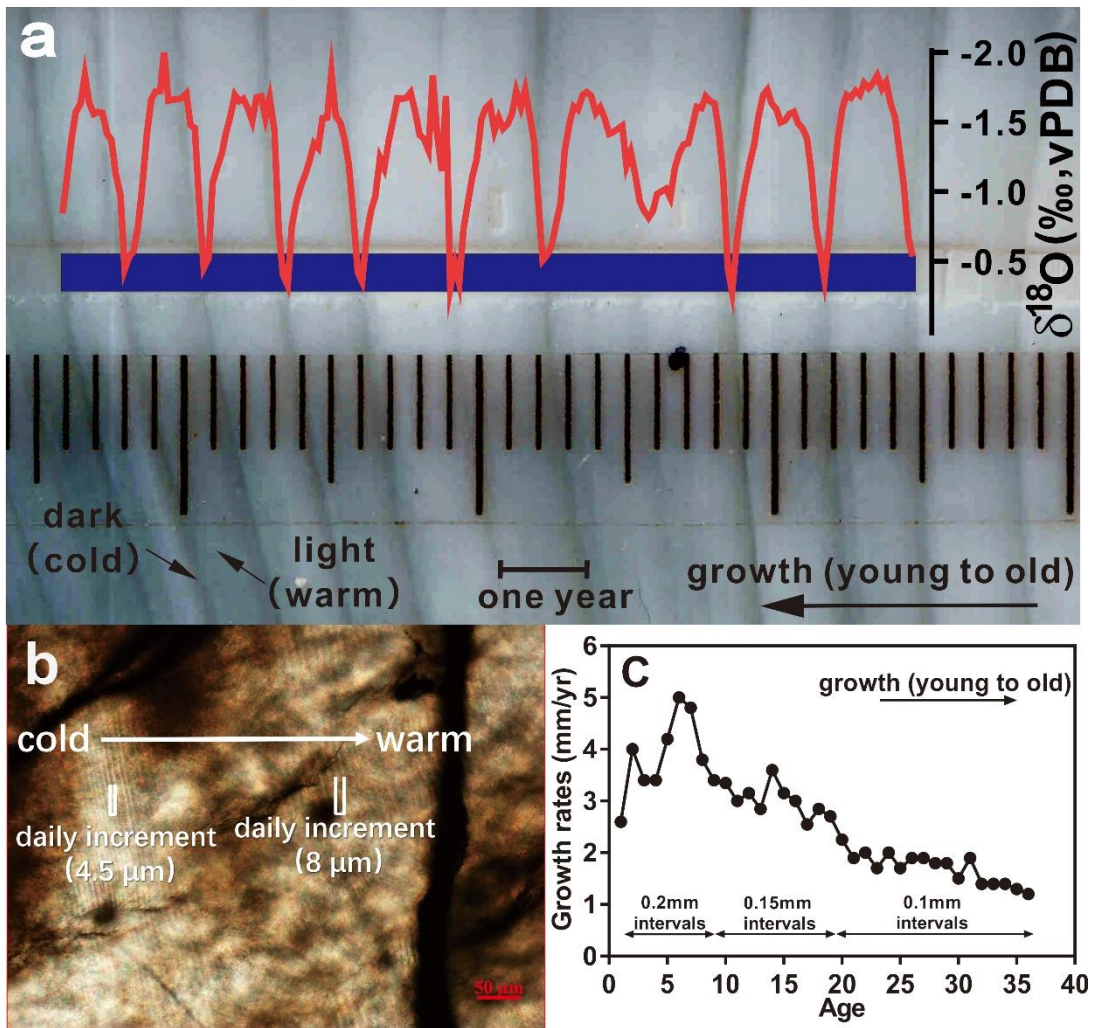
633

634 **Figure 1.** (a) Maps of the South China Sea (source: © Google Maps), with the location of the sample  
 635 study area in the Xisha Islands. (b) Photo of original *Tridacna* A5. A slice was cut through the red  
 636 line of *Tridacna* A5. (c) From the slice, different parts can be seen (hinge, inner layer, and outer  
 637 layer); the red lines are the sampling lines for  $\delta^{18}\text{O}$  analysis. (d) Meteorological observations from  
 638 the Xisha Islands from 1994 to 2005: r-monthly average air temperature (AT) and sea surface  
 639 temperature (SST) with error bars revealing the highest and the lowest temperatures for that  
 640 (e) R-monthly average rainfall and sea surface salinity (SSS) with a standard deviation ( $1\sigma$ ).



641

642 **Figure 2.** (a) The  $\delta^{18}\text{O}$  profiles of A5. (b) The  $\delta^{18}\text{O}_{\text{A5}}$  profiles chronology scale after resampling the  
 643 data; the dotted lines indicate the average annual maximum and minimum.

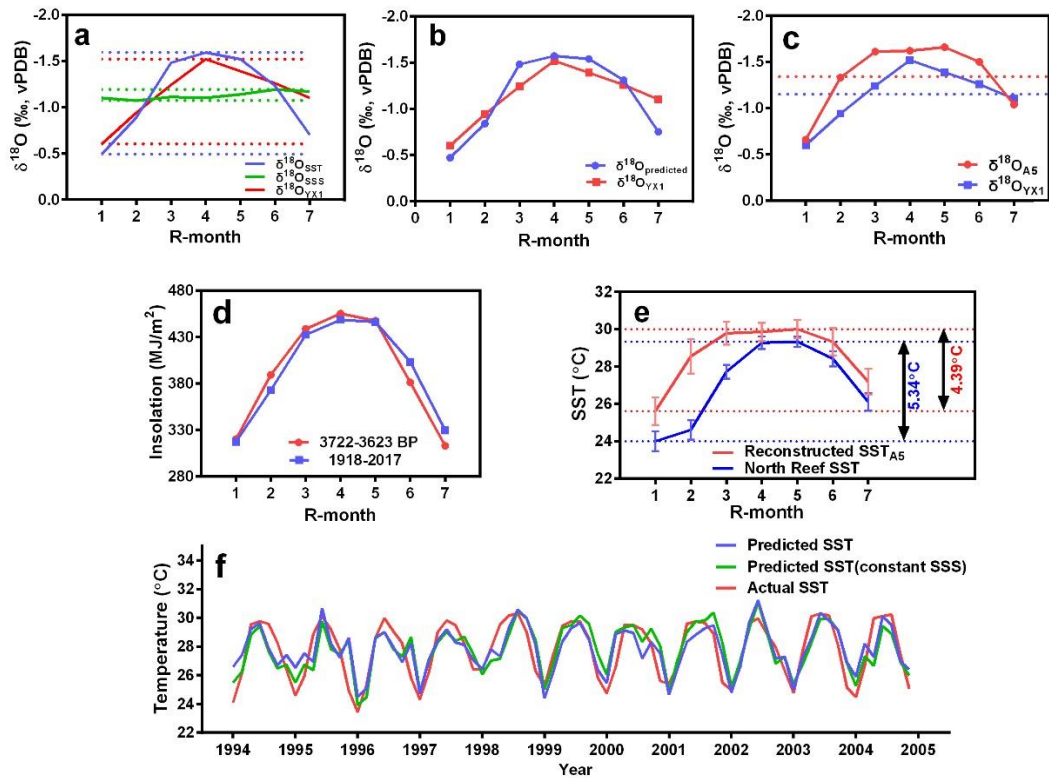


644

645

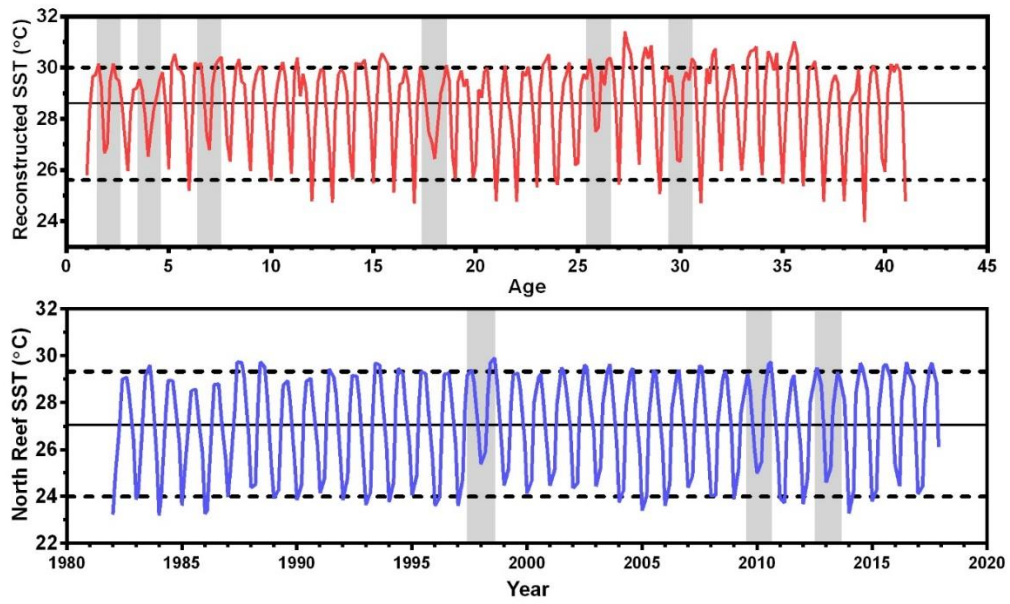
646 **Figure 3.** (a) Dark/bright lines consistent with  $\delta^{18}\text{O}_{\text{A5}}$  profiles. The blue line represents the sampling  
 647 line. Dark and bright lines correspond to high  $\delta^{18}\text{O}$  (cold seasons) and low  $\delta^{18}\text{O}$  (warm seasons),  
 648 respectively. The distance between the dashed lines represents one year, during which the *Tridacna*  
 649 grew. (b) Under the microscope, daily increments (a dark coupled with a bright increment) are  
 650 smaller when temperature is cold, but larger when temperature is higher. (c) Growth rates (line 2 in  
 651 Fig. 1c) in fossil *Tridacna* A5.





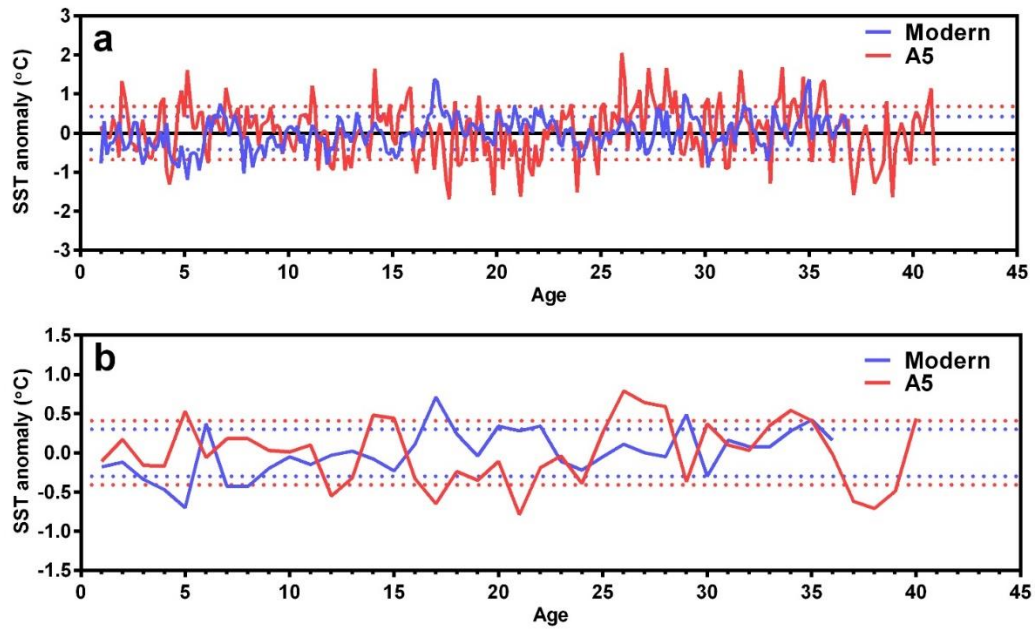
652

653 **Figure 4.** (a) Predicted r-monthly  $\delta^{18}\text{O}$  profiles under constant SSS (blue line) and constant SST  
 654 (green line) conditions, and  $\delta^{18}\text{O}$  of YX1 (red line). Dotted lines represent the maximum and  
 655 minimum of the r-monthly  $\delta^{18}\text{O}$  profiles. (b) R-monthly  $\delta^{18}\text{O}_{\text{YX1}}$  and  $\delta^{18}\text{O}_{\text{predicted}}$ . (c) R-monthly  
 656  $\delta^{18}\text{O}_{\text{YX1}}$  and  $\delta^{18}\text{O}_{\text{A5}}$ , and the dotted lines represent mean values. (d) Different insolation 3700 years  
 657 ago and in **the past** 100 years. (e) Mean seasonal cycles of reconstructed  $\text{SST}_{\text{A5}}$  and North Reef SST.  
 658 (f) Different SST profiles: predicted SST with varied SSS (blue line), constant SSS (green line), and  
 659 actual SST (red line), respectively.



660

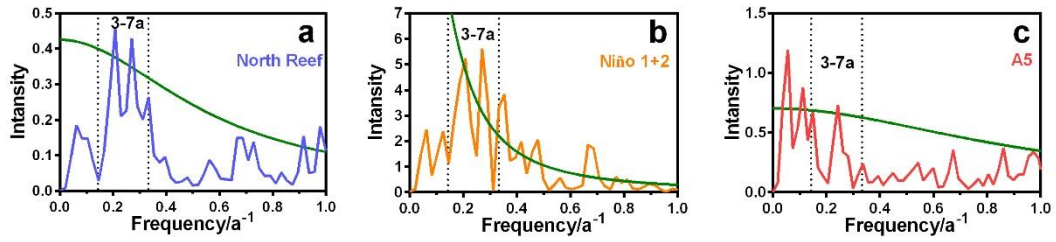
661 **Figure 5.** Reconstructed SST around 3700 years ago (red), compared with the North Reef SST from  
 662 1982 to 2017 (blue). Dotted lines represent the average maximum and minimum SST. The gray field  
 663 represents extreme **El Niño winter events**.



664

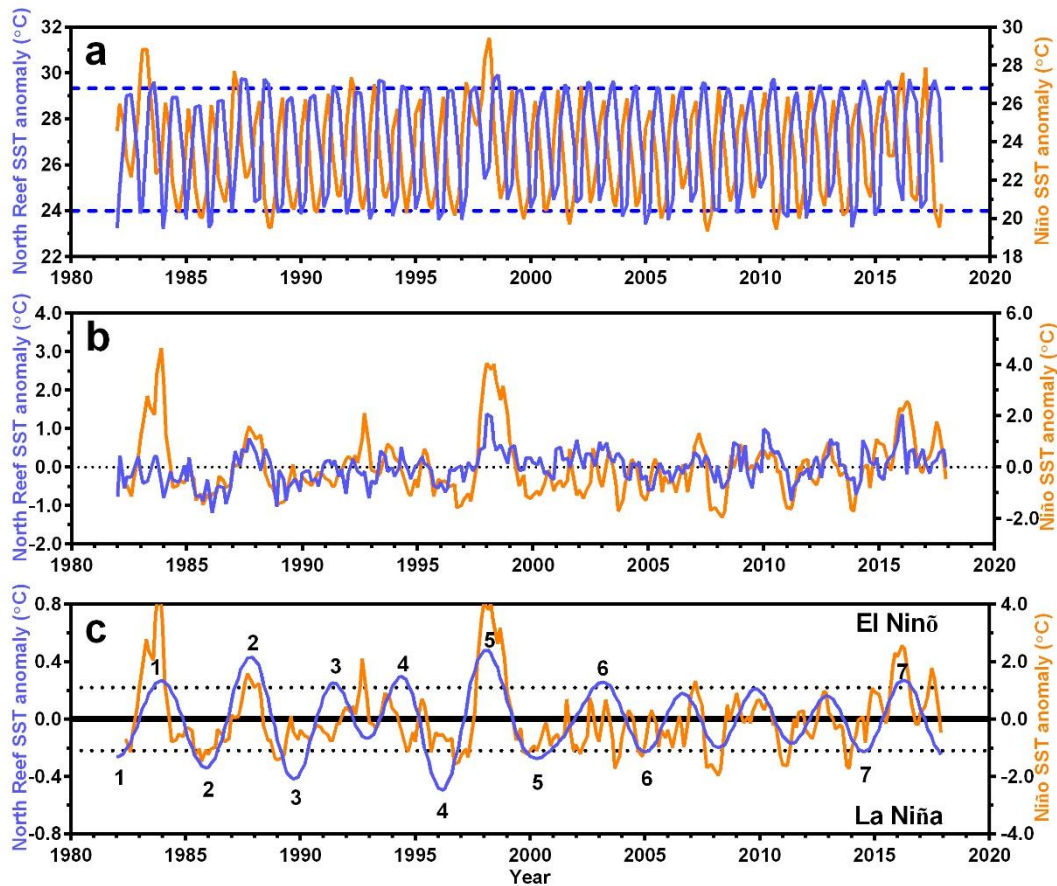
665 **Figure 6.** SST anomalies of modern instrumental data and reconstructed SST anomalies of *Tridacna*  
 666 A5 under r-monthly (a) and r-annual (b) resolution. Dotted lines represent a standard deviation ( $1\sigma$ )  
 667 of SST anomalies.

668



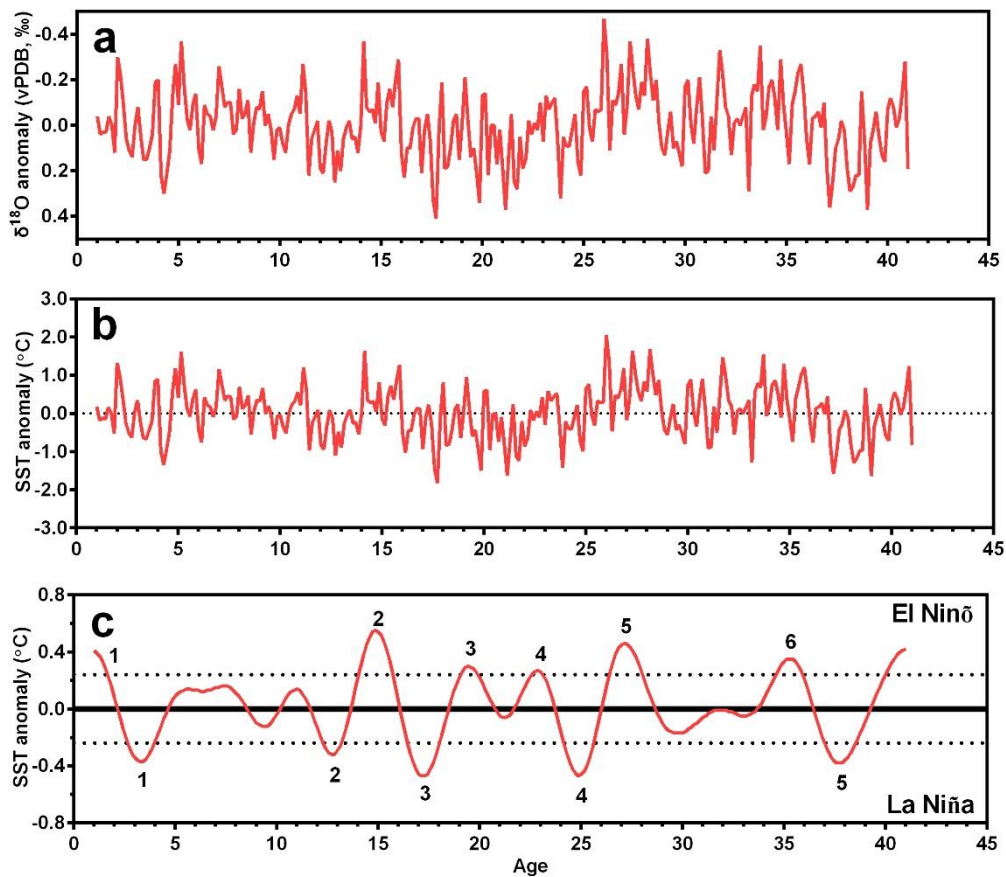
669

670 **Figure 7.** Spectral analysis of the North Reef SST anomalies (a), Niño 1 + 2 SST anomalies (b), and  
 671 reconstructed SST anomalies according to  $\delta^{18}\text{O}_{A5}$  (c). Green lines indicate significance at the 90 %  
 672 confidence level, and the area between the two dotted lines represents the frequency of 3 to 7 years.



673

674 **Figure 8.** Relationship between Niño 1 + 2 SST and the North Reef SST: (a) the North Reef SST  
 675 (blue line) compared with Niño 1 + 2 SST (yellow line); a clear time lag exists. (b) SST anomalies  
 676 of two areas; the lag is removed by forwarding the North Reef SST anomalies for 3 r-months. (c)  
 677 The North Reef SST anomalies performed with 3–7 years of bandpass filtering, consistent with Niño  
 678 1 + 2 SST anomalies; the dashed lines show the calculated threshold limits ( $1\sigma$ ) for ENSO activity  
 679 in the North Reef. El Niño and La Niña events are represented by positive and negative SST  
 680 anomalies values, respectively.



681

682 **Figure 9.** (a) ENSO activity reconstructed by the fossil *Tridacna* 3700 years ago:  $\delta^{18}\text{O}$  anomalies  
 683 of fossil *Tridacna* A5. (b) The North Reef SST anomalies calculated by  $\delta^{18}\text{O}$  anomalies, based on  
 684 modern *Tridacna*  $\delta^{18}\text{O}$ -SST equation ( $1\text{‰ } \delta^{18}\text{O}_{\text{shell}} \approx 4.41^\circ\text{C SST}$ ). (c) ENSO activity according to  
 685 the North Reef SST anomalies after 3-7 years of bandpass filtering; the dashed lines show the  
 686 calculated threshold limits ( $1\sigma$ ) for ENSO activity.